


RESEARCH ARTICLE

p75^{NTR} regulates brain mononuclear cell function and neuronal structure in *Toxoplasma* infection-induced neuroinflammation

Henning Peter Düsedau¹ | Jan Klevevan² | Caio Andreeta Figueiredo¹ | Aindrila Biswas¹ | Johannes Steffen¹ | Stefanie Kliche³ | Stefan Haak² | Marta Zagrebelsky² | Martin Korte² | Ildiko Rita Dunay¹ 

¹Otto-von-Guericke University Magdeburg, Institute of Inflammation and Neurodegeneration, Medical Faculty, Magdeburg, Germany

²Division of Cellular Neurobiology, Zoological Institute, TU Braunschweig, Braunschweig, Germany

³Otto-von-Guericke University, Institute for Molecular and Clinical Immunology, Medical Faculty, Magdeburg, Germany

Correspondence

Ildiko Rita Dunay,
Otto-von-Guericke University Magdeburg,
Institute of Inflammation and
Neurodegeneration, Medical Faculty,
Magdeburg D-39120, Leipziger Str.
44, Germany.
Email: ildikodunay@gmail.com

Funding information

Deutsche Forschungsgemeinschaft, Grant/
Award Number: SFB854, TP25

Neurotrophins mediate neuronal growth, differentiation, and survival via tropomyosin receptor kinase (Trk) or p75 neurotrophin receptor (p75^{NTR}) signaling. The p75^{NTR} is not exclusively expressed by neurons but also by certain immune cells, implying a role for neurotrophin signaling in the immune system. In this study, we investigated the effect of p75^{NTR} on innate immune cell behavior and on neuronal morphology upon chronic *Toxoplasma gondii* (*T. gondii*) infection-induced neuroinflammation. Characterization of the immune cells in the periphery and central nervous system (CNS) revealed that innate immune cell subsets in the brain upregulated p75^{NTR} upon infection in wild-type mice. Although cell recruitment and phagocytic capacity of p75^{NTR} knockout (p75^{-/-}) mice were not impaired, the activation status of resident microglia and recruited myeloid cell subsets was altered. Importantly, recruited mononuclear cells in brains of infected p75^{-/-} mice upregulated the production of the cytokines interleukin (IL)-10, IL-6 as well as IL-1 α . Protein levels of proBDNF, known to negatively influence neuronal morphology by binding p75^{NTR}, were highly increased upon chronic infection in the brain of wild-type and p75^{-/-} mice. Moreover, upon infection the activated immune cells contributed to the proBDNF release. Notably, the neuroinflammation-induced changes in spine density were rescued in the p75^{-/-} mice. In conclusion, these findings indicate that neurotrophin signaling via the p75^{NTR} affects innate immune cell behavior, thus, influencing the structural plasticity of neurons under inflammatory conditions.

KEYWORDS

brain mononuclear cells, chronic *Toxoplasma gondii* infection, dendritic morphology, microglia, neuroinflammation, neurotrophins, p75 neurotrophin receptor, pro-neurotrophins

1 | INTRODUCTION

Neuronal growth, differentiation, survival, and function are orchestrated in the central nervous system (CNS) by neurotrophins—secreted proteins

involved in shaping neuronal connectivity and in repairing the CNS after injury (Kaplan & Miller, 2000). Neurotrophins are initially synthesized as pro-neurotrophins and then cleaved to produce mature proteins. The family of mature neurotrophins includes nerve growth factor (NGF), brain



derived neurotrophic factor (BDNF), Neurotrophin-3 (NT-3), and Neurotrophin-4/5 (NT-4/5). They signal through the tropomyosin receptor kinase (Trk) receptors TrkA, TrkB, TrkC, and the p75 neurotrophin receptor (p75^{NTR}) being a member of the tumor necrosis factor (TNF) receptor family. Neurotrophins are critical mediators of neuronal survival (Chao, 2003). They regulate both the architecture and plasticity of mature CNS neurons and are necessary for learning processes (Zagrebelsky & Korte, 2014). Recently, also the role and function of neurotrophin precursors have been explored with more detail suggesting their important role in injury and disease (Ibáñez & Simi, 2012). Several studies have described that pro-neurotrophins such as proBDNF bind to a heterodimeric receptor complex of p75^{NTR} and sortilin with high affinity inducing cell death and reduced synaptic function (Lee, Kerami, Teng, & Hempstead, 2001; Nykjaer, Willnow, & Petersen, 2005; Woo et al., 2005; Yang et al., 2014). Notably, mature neurotrophins can also influence the immune system, however, little is known about the specific functions in this context. They have been shown to modulate monocyte chemotaxis, to participate in tissue-healing mechanism, suppression of nitric oxide release by microglia (Samah, Porcheray, & Gras, 2008) and to enhance macrophage phagocytic activity (Hashimoto et al., 2005). BDNF produced by microglia cells and T cells (Kruse, Cetin, Chan, Gold, & Lühder, 2007) was able to modulate monocyte and macrophage function, for example, by regulating their differentiation towards tissue macrophages. Vega et al. detected that NGF and BDNF influenced cytokine expression in peripheral blood mononuclear cells (Vega, Garcia-Suarez, Hannestad, Perez-Perez, & Germana, 2003). Furthermore, the conditional depletion of hippocampal BDNF decreased the number of cortical microglia (Braun, Kalinin, & Feinstein, 2017). In this context, p75^{NTR} is of special interest. It is expressed by neurons and also by certain types of immune cells, thus, possibly mediating the interaction between cells of the CNS and the innate immune system under pathological conditions (Meeker & Williams, 2014). However, the role of p75^{NTR} signaling in neuro-immuno-interactions during neuroinflammation has still not been fully elucidated.

The intracellular parasite *Toxoplasma gondii* (*T. gondii*) infects a wide range of hosts worldwide (Hill, Chirukandoth, & Dubey, 2005; Montoya & Liesenfeld, 2004; Munoz, Liesenfeld, & Heimesaat, 2011). Being able to infect all nucleated cells, *T. gondii* spreads throughout the host's body during the acute phase of infection. Eventually, the parasites reach immune-privileged regions such as the CNS. During the chronic phase of infection cysts are predominantly formed in infected neurons enabling the parasites to persist lifelong within the host (Dubey, 1998; Wilson & Hunter, 2004). Chronic infection with *T. gondii* is followed by a Th1 type inflammatory response and cell recruitment to the brain (Biswas et al., 2017; Blanchard, Dunay, & Schlüter, 2015).

Basal neuroinflammation is associated with the latent infection (Hermes et al., 2008). Behavioral changes were reported in *T. gondii*-infected mice, however, the underlying mechanisms are not fully understood (Parlog et al., 2014; Parlog, Schlüter, & Dunay, 2015; Vyas, Kim, Giacomini, Boothroyd, & Sapolsky, 2007). Several factors may be responsible for these alterations such as the specific neuroinflammatory milieu, changes in the neurotransmitter balance affecting neuronal connectivity, or possibly the preference of cysts to specific neuron subtypes. Over the past decades, chronic *Toxoplasma*

infection-induced neuroinflammation has been studied extensively and can, therefore, be employed as a suitable model to investigate immune cell dynamics in the CNS and the interaction between immune cells and neurons.

In a previous study, our research group could highlight the distinct alterations in cortical and hippocampal neurons of mice chronically infected with *T. gondii* (Parlog et al., 2014) showing reduced neuronal connectivity, decreased dendritic complexity, and changes in the synaptic protein expression upon infection. Recently, we further revealed the alterations in the synaptic protein composition induced by chronic *T. gondii* infection (Lang et al., 2018). Moreover, our group was able to show the crucial involvement in host defense by recruited myeloid-derived mononuclear cell subsets to the brain upon chronic toxoplasmosis in addition to tissue resident microglia (Biswas et al., 2015; Möhle et al., 2016; Möhle, Parlog, Pahnke, & Dunay, 2014).

In this study, we set out to investigate the impact of p75^{NTR} signaling on the function of immune cells during cerebral toxoplasmosis and to elucidate the role of p75^{NTR} in mediating the changes in neuronal morphology upon *Toxoplasma*-induced neuroinflammation. Flow cytometric analysis revealed the upregulation of p75^{NTR} surface expression by innate immune cells in the periphery and CNS of wild-type (WT) mice. Although cell recruitment and phagocytic capacity of p75^{NTR} knockout (p75^{-/-}) mice were not altered, the activation status of innate immune cells was modified as indicated by differences in their phenotypic properties. Accordingly, cytokine production by recruited myeloid cells in brains of *T. gondii*-infected p75^{-/-} mice was changed as the anti-inflammatory IL-10 and proinflammatory IL-6 and IL-1 α and were upregulated. Applying Western blot analysis to whole brain lysate we could show a strong increase of proBDNF protein levels in infected WT and p75^{-/-} animals. Finally, changes in spine density were rescued in infected p75^{-/-} mice when compared to WT controls. Taken together, these findings indicate that proBDNF-mediated signaling via the p75^{NTR} affects immune cell activation and neuronal morphology in the brain upon inflammation.

2 | MATERIALS AND METHODS

2.1 | Animals

The experiments were performed using age-matched 2- to 4-month-old female wild-type (WT), Thy1-eGFP-M transgenic (Feng et al., 2000) or p75^{NTR} knockout (p75^{-/-}) C57BL/6 mice. The p75^{-/-} mice were generated in the laboratory of Prof. Georg Dechant (University of Innsbruck, Austria) and were genotyped as previously described (von Schack et al., 2001). C57BL/6 WT were obtained from Janvier (Cedex, France). Thy1-eGFP-M transgenic mice and p75^{-/-} mice and littermate controls were obtained from animal facility at the TU Braunschweig. All animal care was in accordance with institutional guidelines. Food and water were available ad libitum and experiments were performed in accordance to National Institutes of Health (NIH) Guidelines for the Care and Use of Laboratory Animals with local government approval.

2.2 | Infection

For the infection of mice with *T. gondii*, cysts of the type II strain ME49 were first collected from brains of female NMRI mice infected with *T. gondii* cysts 10–12 months earlier as described before (Möhle et al., 2016). Each animal was infected with a dose of 2 cysts intraperitoneally while naive control animals were mock infected with sterile Phosphate buffered saline (PBS). Mice were sacrificed 4 weeks post infection (p.i.).

2.3 | Tissue preparation and analysis of neuronal morphology

All mice were transcardially perfused with 4% Paraformaldehyde (PFA), the brain was postfixed and the hemispheres were sliced at 300 μm (for reconstruction of the dendrites) or 150 μm (for spine density analysis) with a vibratome (VT 1200S; Leica) and mounted with an anti-fading mounting medium. To analyze dendritic architecture, hippocampal CA1 neurons were imaged using a 20x (NA 0.8) objective for acquiring z-stacks (step size 1 μm). Only isolated, not overlapping eGFP expressing hippocampal CA1 neurons were chosen. Morphological analysis was performed using Neurolucida[®] (Microbrightfield Bioscience) to trace the dendritic tree and perform a Sholl analysis of dendritic complexity (Sholl, 1953). To analyze dendritic spine density, z-stacks of mid-apical dendrites from hippocampal CA1 and cortical layer V/VI pyramidal neurons were acquired using a 40x oil objective (NA 1.3) with z-steps of 0.5 μm . The number of spines and the dendritic length was analyzed on three-dimensional images using ImageJ software using the multipoint tool and the segmented line respectively. The experimenter was blind to the genotype and treatment throughout all phases of the experiment and analysis.

2.4 | Immunohistochemistry

After fixation by perfusion, as above, the hippocampi were dissected, postfixed in 4% PFA and subsequently cryoprotected. The hippocampi were cryo-sectioned at 30 μm and after a blocking and permeabilization step the sections were incubated overnight with anti-Iba1 primary antibodies (dilution of 1:1,000; Synaptic Systems, #234003), then with a Cy3-conjugated goat anti-rabbit IgG (1:500, Dianova) and mounted using an anti-fading mounting medium. For analyzing changes in microglia density z-stacks of 3 to 5 regions of interest (ROIs) per mouse were imaged using a 20x objective (NA 0.8) at a z-step of 1 μm . The number of microglia was counted using the multipoint tool of ImageJ and is expressed as number of cells per mm^3 of tissue. For analyzing the enwrapping of microglia around neuronal cell bodies, confocal images of at least 10 randomly selected eGFP-expressing CA1 pyramidal neurons were analyzed with a BX61WI FluoView 1000 (FV1000) Olympus confocal microscope. Stacks were acquired using a 40x oil objective (NA 1.3), z-steps of 1 μm . The neuron profile as well as the length of Iba1 positive microglia processes contacting the neuronal cell body were measured using the freehand tool from ImageJ for each z-plane and summed to obtain one value of overlap per each neuron (expressed in % of the neuronal perimeter).

2.5 | Cell isolation

Blood of mice was collected and prepared as described before (Biswas et al., 2015). Brains were collected from mice previously perfused intra-cardially with sterile PBS. Obtained samples were homogenized in a buffer containing HBSS (Gibco), 1M HEPES (pH 7.3, Thermo Fisher) and 45% glucose before sieving through a 70 μm cell strainer. The homogenate was fractionated on a discontinuous 30–70% Percoll gradient (GE Healthcare) and collected cells were washed in PBS and used subsequently for further experiments. To isolate peripheral immune cells, spleens of mice were passed through a 40 μm cell strainer followed by a lysis of erythrocytes in RBC lysis Buffer (eBioscience). Cells were pelleted and stored in -80°C until further use.

2.6 | Flow cytometric analysis

For flow cytometric analysis of cell phenotypes, isolated cells were first incubated with Zombie NIR[™] or Zombie Violet[™] fixable dye (Biolegend) for live/dead discrimination and with anti-Fc γ III/II receptor antibody (clone 93) to prevent unspecific binding of antibodies. Cells were further stained with fluorochrome-conjugated antibodies against cell surface markers in FACS buffer containing 2% fetal bovine serum and 0.1% sodium azide. CD45 (30-F11), CD11b (M1/70), Ly6C (HK1.4), MHCII I-A/I-E (M5/114.15.2), CD4 (GK1.5), CD8 (53–6.7), CD11c (N418), CD80 (16-10A1), and F4/80 (BM8) were all purchased from eBioscience. Ly6G (1A8), CD3 (17A2), and CD25 (3C7) were purchased from Biolegend and p75^{NTR} (MLR2) was bought from Thermo Fisher. Fluorescence Minus One (FMO) controls were used to determine the level of autofluorescence.

For flow cytometric analysis of intracellular cytokines and proteins, single cell suspensions of brains from infected animals were restimulated with 0.21 $\mu\text{g}/\mu\text{l}$ *Toxoplasma* lysate antigen in a 96-well plate (5×10^5 cell/well) for 6 hr. After 2 hr of incubation, Brefeldin A (10 $\mu\text{g}/\text{ml}$, GolgiPlug, BD Biosciences) and Monensin (10 $\mu\text{g}/\text{ml}$ Golgi-Stop, BD Biosciences) were added. Thereafter, cells were incubated with ZOMBIE NIR[™] or Violet[™] fixable dye and anti-Fc γ III/II receptor antibody. Next, surface staining was performed on the cells with antibodies for CD45 (30-F11), CD11b (M1/70), Ly6C (HK1.4), Ly6G (1A8), CD3 (17A2), CD4 (GK1.5), CD8 (53–6.7), in FACS buffer. Cells were fixed in 4% paraformaldehyde and then permeabilized using Permeabilization Buffer (Biolegend). Intracellular cytokines and proteins were stained with fluorochrome-conjugated antibodies: IL-1 α (ALF-161), IL-1 β (NJTEN3), IL-6 (MP5-20F3), IL-10 (JES5-16E3), IL-12 (C17.8), purchased from eBiosciences; iNOS (BD Biosciences, 610330) in Permeabilization Buffer. Matched isotype controls were used to assess the level of unspecific binding.

A minimum of 100,000 cells were acquired using the BD FACS Canto II and Thermo Fisher Attune NxT flow cytometer. Obtained data were analyzed using FlowJo software (Version 10 Tree Star).

2.7 | Ex vivo phagocytosis assay

Isolated cells from brains of infected mice were transferred into wells of a 96-well plate (4×10^5 cells/well) and incubated at 37°C for 1 hr. Negative controls were set up by treatment of cells with cytochalasin D

(Sigma) for 30 min before FITC-fluorescent, carboxylated latex beads were added ($d = 1 \mu\text{m}$, Fluospheres, Thermo Fisher). Next, cells were washed twice and stained for flow cytometric analysis. Phagocytosis of beads by each cell population was determined using the BD FACS Canto II flow cytometer and obtained data were analyzed using FlowJo software (Version 10 Tree Star).

2.8 | In vitro migration assay

Isolated blood cells were washed in RPMI (Gibco) medium containing 10 mM HEPES (Sigma) and 0.1% bovine serum albumin (pH 7.4) before being transferred into a Transwell insert (3×10^5 cells/well, Costar Corning) previously coated with recombinant human Fc-tagged murine VCAM (5 $\mu\text{g}/\text{ml}$, R&D systems) in PBS. The inserts were then placed on a 24-well plate filled with RPMI medium (10 mM HEPES, 0.1% BSA, pH 7.4), with or without stimulation of mCCL2 (20 ng/ml, R&D systems). After 2 hr incubation at 37 °C and 5% CO₂, cells were isolated from the lower compartment and counted under a light microscope.

2.9 | Western blot analysis

For Western blot analysis, proteins were either isolated from whole mouse brains or spleenocytes obtained previously. In the case of brain samples, collected tissue was immediately snap frozen in liquid nitrogen and stored in -80 °C until further preparation. In all cases, samples were lysed on ice in RIPA lysis buffer containing protease inhibitors, 50 mM Tris/HCl (pH 7.4); 150 mM NaCl; 1% IGEPAL CA-630; 0.25% Na-deoxycholate; 1 mM NaF. Proteins were separated by SDS-polyacrylamide gel electrophoresis (12.5%) and transferred to nitrocellulose. Membranes were incubated overnight at 4 °C in a 1:500 dilution of anti-BDNF antibody (abcam, #203573) or 1:000 dilution of anti-NFG antibody (abcam, #52918), respectively. As a loading control the same membrane was incubated with a 1:1,000 dilution of anti- β -Tubulin-III antibody (Sigma, #T8660) or, for immune cells derived from spleens, with GAPDH 1:1,000 (Cell signaling, #2118S). Bound antibodies were revealed using enhanced chemiluminescence assay and densitometric analysis of blots was performed using ImageJ with Fiji distribution (Schindelin et al., 2012).

2.10 | Statistics

Data from flow cytometry, RT-PCR and Western blot analysis were analyzed by Mann-Whitney test for two groups or one-way and two-way ANOVA for several groups followed by Tukey's post hoc HSD test with GraphPad Prism 6 (San Diego, CA). The Sholl analysis data were analyzed applying a two-tailed Student's *t* test point by point. Total complexity and spine density were compared between groups using a one-way ANOVA followed by a post hoc Tukey's HSD test. In all cases, results were presented as mean \pm standard error of the mean (SEM) and were considered significant, with $p < .05$.

3 | RESULTS

3.1 | Infection with *T. gondii* upregulates p75^{NTR} on innate immune cells in the brain

The first aim of this study was to investigate the level of p75^{NTR} surface expression on innate immune cells in steady state and upon inflammation. Therefore, we analyzed isolated cells from the blood and brain of naive and *T. gondii*-infected C57BL/6 WT mice by flow cytometry. In the blood of noninfected mice, we already observed a large number of Ly6C^{hi} monocytes (71.5 \pm 6.5%) and Ly6C^{low} macrophages (73.1 \pm 0.6%) expressing p75^{NTR} whereas Ly6C^{int} blood monocytes expressed the neurotrophin receptor to a lesser extent (39.4 \pm 2.0%; Figure 1c). Upon infection, the cellular expression of p75^{NTR} by mononuclear cells in the blood was increased on all subsets (Ly6C^{hi} monocytes: 71.5 \pm 6.5% vs. 83.7 \pm 0.7%; $p < .14$ / Ly6C^{int} blood monocytes: 39.4 \pm 2.0% vs. 51.6 \pm 3.4%; $p < .07$ / Ly6C^{low} macrophages: 73.1 \pm 0.6% vs. 83.1 \pm 1.6%; $p < .04$). Next, we analyzed immune cells isolated from the brains of noninfected and *T. gondii*-infected WT mice (Figure 1d, d'). Considering the low number of recruited myeloid cells with approximately 1% of living single cells in the CNS under steady state condition (data not shown) the corresponding flow cytometric histograms are not representative (Figure 1d). In control brains a small proportion of microglia cells expressed p75^{NTR} (21.4 \pm 1.3%). Upon infection, the amount of microglia and recruited myeloid cells expressing p75^{NTR} increased (microglia: 21.4 \pm 1.3% vs. 94.2 \pm 1.2%; $p < .04$ / myeloid cells: 37.3 \pm 5.3% vs. 85.0 \pm 1.3%; $p < .04$). Among the myeloid cell subsets, Ly6C^{hi} monocytes and Ly6C^{int} brain DCs displayed similar surface expression of the neurotrophin receptor (Ly6C^{hi} monocytes: 20.3 \pm 12.8% vs. 86.8 \pm 1.2%; $p < .04$ / Ly6C^{int} brain DCs: 47.9 \pm 11.4% vs. 87.1 \pm 1.0%; $p < .04$) and the subset of Ly6C^{low} macrophages increased their p75^{NTR} surface expression the greatest (47.4 \pm 2.8% vs. 94.7 \pm 1.3%; $p < .04$) but the receptor was not detected on recruited lymphocytes (1.8 \pm 0.6% vs. 6.2 \pm 0.8%; $p < .04$). When comparing the median fluorescence intensity (MFI) of the p75^{NTR} expression level between microglia and recruited myeloid cells in the CNS we could show that expression of p75^{NTR} was similar between peripheral innate immune cells and brain resident immune cells (Figure 1e). Taken together, our results indicate the upregulation of p75^{NTR} by innate immune cells in the blood and CNS upon *T. gondii* infection.

3.2 | Knockout of p75^{NTR} does not affect cell recruitment during *T. gondii* infection

To elucidate the effect of p75^{NTR} on the behavior of immune cells we utilized p75^{NTR}^{RexonIV} knockout (p75^{-/-}) mice. Due to the strong expression of the neurotrophin receptor on peripheral blood mononuclear cells we first aimed to analyze the potential effect of p75^{NTR} on immune cell trafficking. Thus, we infected p75^{-/-} and WT mice with *T. gondii* and analyzed the composition of immune cells in the hippocampus and cortex by flow cytometry (Figure 2a-c). When compared to WT animals, no difference was observed in the composition of brain resident microglia cells in cortex (WT: 22.5 \pm 2.3% vs. p75^{-/-}:

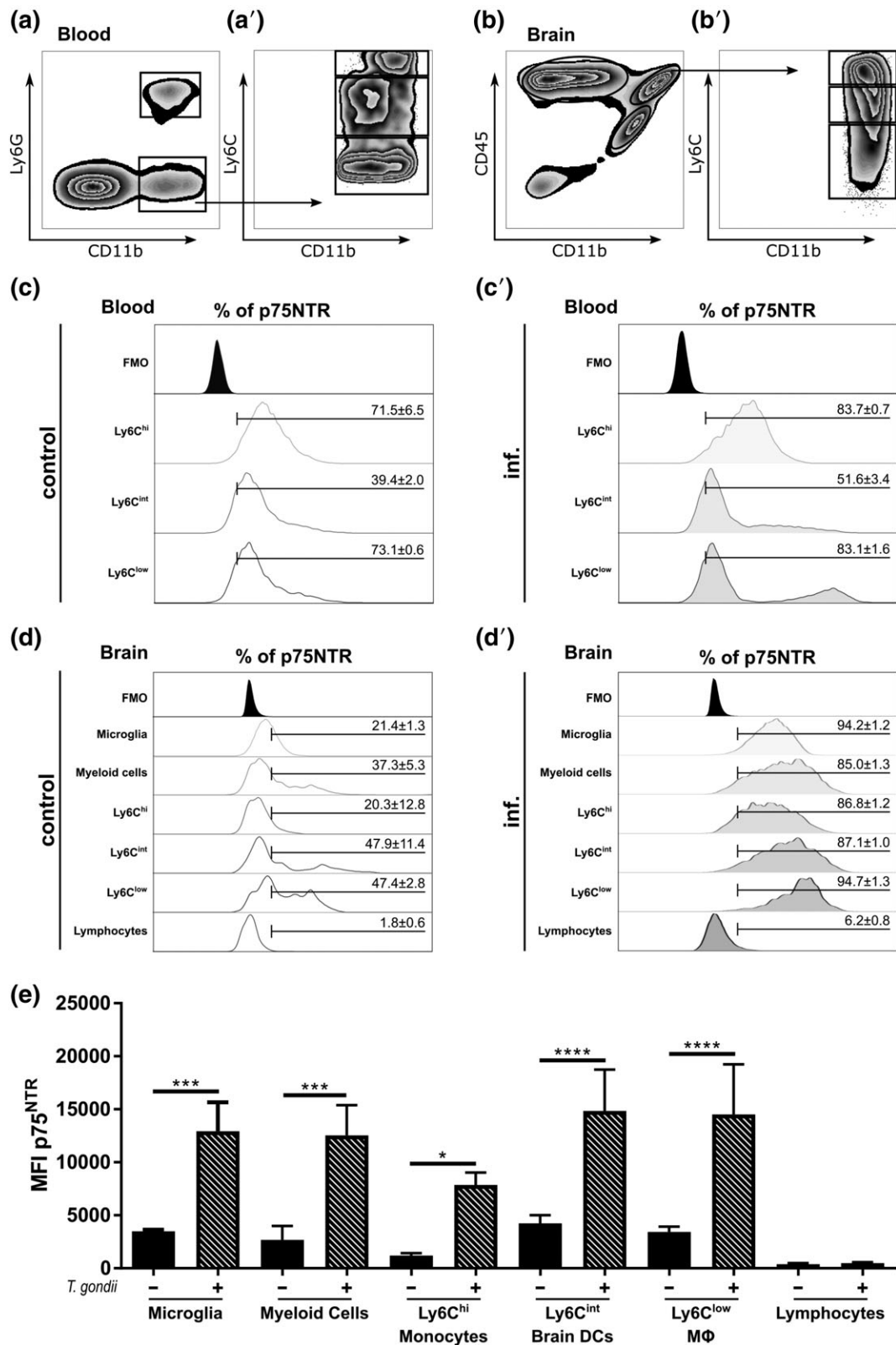


FIGURE 1 Flow cytometric analysis of p75^{NTR} surface expression on immune cells upon infection with *T. gondii*. Cells were isolated from blood and brains of noninfected and *T. gondii*-infected mice then analyzed by flow cytometry. (a, a') Representative gating strategy for myeloid cells from blood of animals infected with *T. gondii*. Cells were selected based on the forward-scatter/side-scatter plot (FSC/SSC), dead cells were excluded and only single cells were selected for further analysis (not shown). (a) Neutrophil granulocytes (CD11b⁺Ly6G⁺) in the blood were excluded (upper gate) and monocytes remained as CD11b⁺Ly6C⁻ cells (lower gate). (a') Monocytes were further divided with respect to the surface expression of Ly6C into CD11b⁺Ly6C^{hi} inflammatory monocytes (upper gate), CD11b⁺Ly6C^{int} blood monocytes (middle gate) and CD11b⁺Ly6C^{low} resident macrophages (bottom gate). (b, b') Representative gating strategy for immune cells isolated from the brain of animals infected with *T. gondii*. After FSC/SSC gating, dead cells were excluded and only single cells were selected for further analysis (not shown). (b) Based on the expression of CD45 and CD11b, CD45⁺CD11b^o lymphocytes (upper left gate), CD45⁺CD11b^{hi} myeloid cells (upper right gate)

and CD45^{int}CD11b^{int} microglia (lower right gate) were identified. Next, neutrophil granulocytes were excluded from the myeloid cell population by their expression of CD11b and Ly6G (not shown). (b') Myeloid cells were further divided into CD11b⁺Ly6C^{hi} inflammatory monocytes (upper gate), CD11b⁺Ly6C^{int} monocyte-derived DCs (middle gate) and CD11b⁺Ly6C^{low} monocyte-derived macrophages (bottom gate; Biswas et al., 2015). The lymphocyte population was subdivided into CD3⁺CD4⁺ T cells and CD3⁺CD8⁺ T cells (data not shown). Surface expression of p75^{NTR} was analyzed on blood cells (c) and brain cells (d) of noninfected mice and on blood cells (c') and brain cells (d') of animals infected with *T. gondii*. Cell populations were selected as described above and histograms show the representative expression level of p75^{NTR} by the cell population in comparison to the corresponding FMO control. Bars mark cells positively expressing p75^{NTR} and numbers above bars represent the percentage of cells (\pm SEM) in the respective population. (e) Flow cytometric analysis of p75^{NTR} surface expression on cells isolated from brains of naive and *T. gondii*-infected mice. Cell populations were selected as described above and bar charts display the median fluorescence intensity (MFI; \pm SEM). Differences between groups were analyzed by one-way ANOVA with post hoc Tukey's HSD test (* $p < .05$; *** $p < .001$; **** $p < .0001$)

20.8 \pm 1.9%; $p < .98$) or hippocampus (WT: 32.5 \pm 4.4% vs. p75^{-/-}: 32.0 \pm 2.8%; $p < .99$) of p75^{-/-} mice. Further, the knockout of p75^{NTR} did not result in an altered recruitment of myeloid cells from the periphery to the cortex (WT: 13.7 \pm 0.8% vs. p75^{-/-}: 10.7 \pm 1.0%; $p < .59$) or hippocampus (WT: 17.8 \pm 1.5% vs. p75^{-/-}: 14.8 \pm 2.7%; $p < .6$) of infected mice. In accordance to these findings, no differences were found in the composition of lymphocytes in cortex (WT: 34.8 \pm 3.6% vs. p75^{-/-}: 39.3 \pm 2.0%; $p < .66$) or hippocampus (WT: 37.3 \pm 3.5% vs. p75^{-/-}: 44.0 \pm 0.8%; $p < .34$). Next, we addressed whether p75^{NTR} knockout affects the migratory response of immune cells. Therefore, an in vitro migration assay was employed with isolated leukocytes from WT and p75^{-/-} mice and compared the total number of migrated cells with or without stimulation by the chemokine CCL2 (Figure 2d). In unstimulated samples, no differences in the migration of immune cells from WT (0.22 $\times 10^4$ cells/ml \pm 0.037 $\times 10^4$ cells/ml) or p75^{-/-} mice (0.23 $\times 10^4$ cells/ml \pm 0.018 $\times 10^4$ cells/ml; $p < .99$) were detected. Upon administration of CCL2, the total number of migrated cells strongly increased for both groups, however, no alterations were observed between WT (0.72 $\times 10^4$ cells/ml \pm 0.034 $\times 10^4$ cells/ml) and knockout animals (0.72 $\times 10^4$ cells/ml \pm 0.021 $\times 10^4$ cells/ml; $p < .99$). In summary, knockout of the p75^{NTR} did not have an impact on the recruitment of immune cells to the CNS and did not lead to differences in the migratory response of leukocytes.

3.3 | Phenotypic characterization of innate immune cells in the CNS of p75^{-/-} mice upon *T. gondii*-induced neuroinflammation

Although no change was detected in the composition of immune cells in the brains of p75^{-/-} mice, we characterized phenotype and activation status of the cell subsets upon *T. gondii*-induced neuroinflammation. Flow cytometric analysis was performed to assess the expression level of distinct surface markers by immune cell subsets isolated from infected brains of WT and p75^{-/-} mice. When compared to WT, brain resident microglia from p75^{-/-} animals showed a significantly reduced MFI for Major Histocompatibility complex (MHC) class II surface expression ($p < .02$), CD11c ($p < .01$) and co-stimulatory CD80 ($p < .03$), as indicated in Figure 3a–d. The histograms show that the subsets expressing the indicated markers were similar between the experimental groups for MHC class II (WT: 95.8 \pm 0.5% vs. p75^{-/-}: 98.6 \pm 0.5%; $p < .09$) and CD11c (WT: 89.9 \pm 2.9% vs. p75^{-/-}: 91.4 \pm 1.1%; $p < .86$). Yet CD80 was found to be expressed by fewer cells in p75^{-/-} samples (WT: 94.5 \pm 0.4% vs. p75^{-/-}: 88.6 \pm 1.2%; $p < .02$; Figure 3a'–d'). In contrast to microglia, Ly6C^{hi} monocytes showed no differences between p75^{-/-} and WT animals with respect to MFI values or expressing cell fractions for the surface markers MHC II, CD11c, F4/80, and CD80 (Figure 3e–h'). As we reported previously, peripheral Ly6C^{hi} inflammatory monocytes enter the parenchyma and differentiate into Ly6C^{int} brain dendritic cells (DCs) and

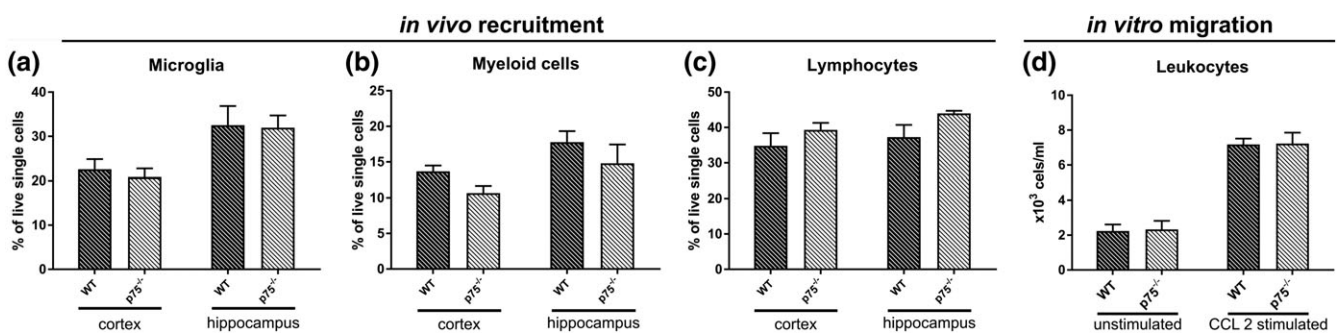


FIGURE 2 Immune cell recruitment to cortex and hippocampus of WT and p75^{-/-} mice upon infection with *T. gondii* and in vitro leukocytes migration (a–c) the composition of immune cells isolated from cortices and hippocampi of *T. gondii*-infected WT and p75^{-/-} mice was determined by flow cytometric analysis. Cell populations were gated as described in Figure 1b,b' and bar charts display the fraction of each population as frequency of living single cells (\pm SEM). (d) The migratory response of leukocytes from *T. gondii*-infected WT and p75^{-/-} mice was assessed in vitro by a transwell migration assay. Isolated cells were either stimulated with the chemokine CCL2 or were left unstimulated. Bar charts represent the mean of total cell count (\pm SEM) in the compartment below the membrane. Differences between groups were analyzed by two-way ANOVA with post hoc Tukey's HSD test

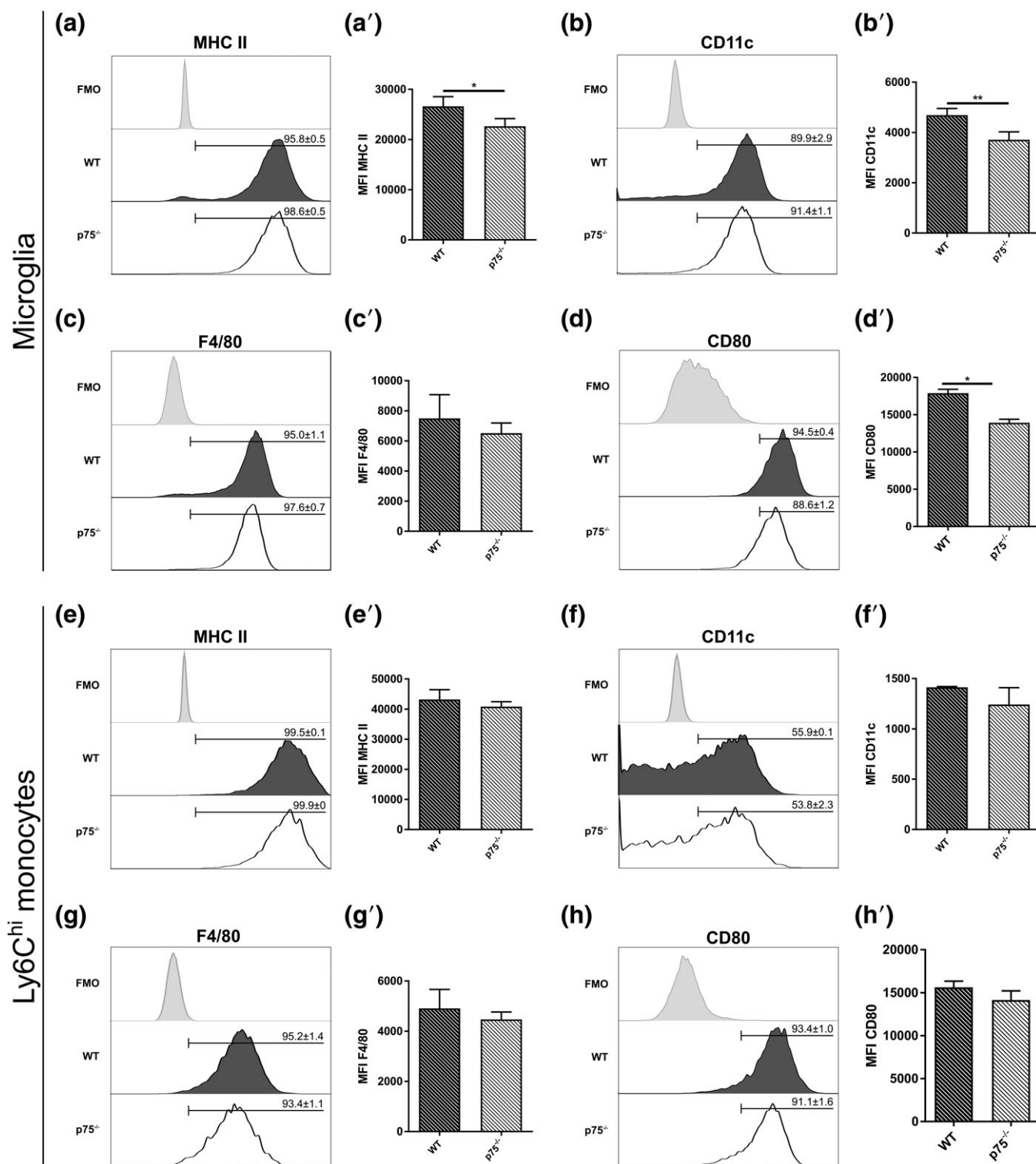


FIGURE 3 Phenotypic analysis of activated microglia and Ly6C^{hi} monocytes from brains of *T. gondii*-infected WT and p75^{-/-} mice. The surface expression of activation markers on cells isolated from infected brains of WT and p75^{-/-} mice was determined by flow cytometric analysis. Cell populations were selected as described in Figure 1b, b'. (a–h) Histograms show the representative expression level of the surface marker by cells (WT mice tinted, p75^{-/-} mice without tint) in comparison to the corresponding FMO control and bars mark cells positively expressing the surface marker. Numbers above bars represent the percentage of cells (±SEM) in the respective population. (a'–h') Bar charts display the MFI (±SEM) for the specific surface marker. Differences between groups were analyzed by Mann–Whitney test (**p* < .05, ***p* < .01)

Ly6C^{low} macrophages (Biswas et al., 2015). Interestingly, Ly6C^{int} brain DCs in p75^{-/-} animals displayed a significant reduction in the MFI of CD11c (*p* < .002) although the fraction of expressing cells was not changed (WT: 83.9 ± 0.1% vs. p75^{-/-}: 78.0 ± 1.4%; *p* < .1;

Figure 4c). In accordance to this, knockout of p75^{NTR} also resulted in a diminished MFI for CD11c (*p* < .03) and F4/80 (*p* < .001) surface expression levels on Ly6C^{low} macrophages (Figure 4e–h') but not in cells positively expressing the respective surface receptors (CD11c:

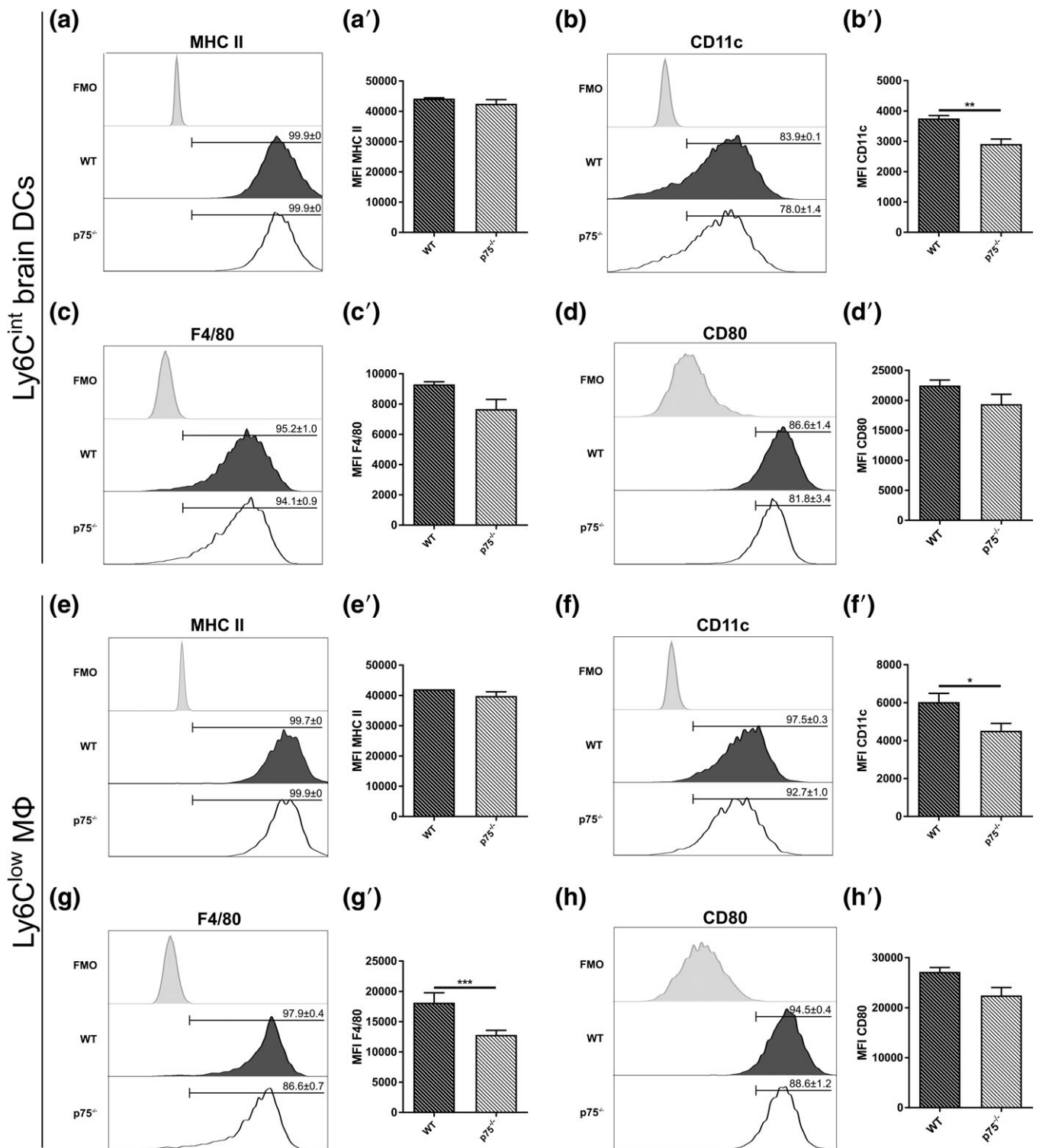


FIGURE 4 Phenotypic analysis of activated Ly6C^{int} brain DCs and Ly6C^{low} macrophages from brains of *T. gondii*-infected WT and p75^{-/-} mice. The surface expression of activation markers on cells isolated from infected brains of WT and p75^{-/-} mice was determined by flow cytometric analysis. Cell populations were selected as described in Figure 1b, b'. (a-h) Histograms show the representative expression level of the surface marker by cells (WT mice tinted, p75^{-/-} mice without tint) in comparison to the corresponding FMO control and bars mark cells positively expressing the surface marker. Numbers above bars represent the percentage of cells (±SEM) in the respective population. (a'-h') Bar charts display the MFI (±SEM) for the specific surface marker. Differences between groups were analyzed by Mann-Whitney test (* $p < .05$, ** $p < .01$, *** $p < .001$)

WT: $97.5 \pm 0.3\%$ vs. p75^{-/-}: $92.7 \pm 1.0\%$; $p < .1$ / F4/80: WT: $97.9 \pm 0.4\%$ vs. p75^{-/-}: $86.6 \pm 0.7\%$; $p < .24$). We further investigated the CD4⁺ and CD8⁺ T cell lymphocyte populations and quantified their activation status in infected brains of WT and p75^{-/-}

animals by flow cytometric analysis (Supporting Information 1A-C'). The frequencies of CD4⁺ T cells (WT: $50.8 \pm 1.2\%$ vs. p75^{-/-}: $52.0 \pm 2.3\%$; $p < .74$) and CD8⁺ T cells (WT: $46.4 \pm 1.3\%$ vs. p75^{-/-}: $45.1 \pm 2.2\%$; $p < .86$) in *T. gondii*-infected brains were not differing

between p75^{-/-} and WT mice. Interestingly, significantly less CD4⁺ T cells in p75^{-/-} mice were expressing the IL-2 receptor alpha chain CD25 (WT: 13.6 ± 0.2% vs. p75^{-/-}: 11.4 ± 0.1%; $p < .03$) which also resulted in a significantly lower MFI ($p < .03$). CD8⁺ T cells of both experimental groups expressed CD25 equally (WT: 12.2 ± 1.2% vs. p75^{-/-}: 9.9 ± 0.8%; $p < .34$) and did not show significant differences in MFI. In conclusion, the phenotypic analysis of brain resident and recruited peripheral immune cells during cerebral toxoplasmosis revealed several differences between p75^{-/-} and WT animals implying a modified activation of the immune cells in knockout animals.

3.4 | Knockout of p75^{NTR} has no effect on phagocytic capacity but alters intracellular cytokine production by innate immune cells

To further examine whether the function of immune cells in p75^{-/-} mice could also be affected, an ex vivo phagocytosis assay was performed. For that reason, resident, and recruited immune cells from infected brains were isolated and subsequently incubated with FITC-fluorescent latex beads. The MFI of each population in the FITC detection channel was determined by flow cytometry and results were compared between WT and p75^{-/-} mice (Figure 5a). The results reveal, that phagocytic activity of microglia or recruited myeloid cell populations in p75^{-/-} mice and WT cells was not distinct.

Next, the morphological activation of microglia was assessed by analyzing their structural alterations and density. Under steady state conditions, in both WT and p75^{-/-} mice the microglia in the CA1 region of the hippocampus showed the ramified morphology, typical for resting cells (Figure 5b above). Upon *T. gondii* infection, microglia transformed their morphology to an activated amoeboid form with hypertrophic processes that tightly wrap around the cell bodies and main dendrites of eGFP-positive CA1 pyramidal neurons (Figure 5b below and 5b'). We further quantified the overlay between Iba1⁺ microglial processes and the perimeter of eGFP expressing pyramidal neurons and observed a significant increase upon *T. gondii* infection (Figure 5c; WT: $p < .001$; p75^{-/-}: $p < .001$). The increase in microglia/neuron overlap was not significantly different in p75^{-/-} when compared to WT infected mice (Figure 5c). Finally, microglia density was quantified and showed an equally significant increase in the number of Iba1⁺ microglia cells in the CA1 region of p75^{-/-} and WT infected mice (Figure 5d; WT $p < .001$; p75^{-/-} $p < .001$). Taken together, the results show a strong activation of microglia upon *T. gondii* infection that does not significantly differ between WT and p75^{-/-} mice.

In the next step, we focused on the flow cytometric analysis of cytokine expression by immune cell populations in brains of *T. gondii*-infected animals. Upon in vitro re-stimulation with *Toxoplasma* lysate antigen (TLA) the production of IL-1 α , IL-6, and IL-10 by microglia from WT and p75^{-/-} mice did not differ (Figure 6a-d'). Interestingly, a significantly higher percentage of Ly6C^{hi} monocytes from p75^{-/-} animals expressed IL-1 α when compared to WT samples (WT: 32.1 ± 1.8% vs. p75^{-/-}: 48.7 ± 3.1%; $p < .0001$) despite MFI values being similar ($p < .2$; Figure 6e, e'). Moreover, p75^{NTR} knockout resulted in an increased MFI of IL-10 ($p < .03$) but not in a higher number of Ly6C^{hi} monocytes expressing this cytokine (WT: 0.5 ± 0.2% vs. p75^{-/-}: 1.2 ± 0.2%; $p < .99$; Figure 6h, h'). Similarly,

analysis of Ly6C^{int} brain DCs reported significantly higher fluorescence intensities for IL-10 ($p < .03$) and also IL-6 ($p < .03$) in infected p75^{-/-} animals while the frequency of secreting cells did not differ (Figure 7a-d'). We also discovered an increased percentage of Ly6C^{low} macrophages from p75^{-/-} mice secreting IL-1 α (WT: 26.3 ± 1.7% vs. p75^{-/-}: 38.6 ± 3.2%, $p < .0004$), resulting in significantly higher median fluorescence ($p < .03$). In addition, significantly elevated MFIs were also detected for IL-6 ($p < .03$) and IL-10 ($p < .3$) when compared to WT samples while positively expressing cell fractions were not altered (Figure 7e-h'). Levels of IL-12 and inducible nitric oxide synthase (iNOS) in microglia and recruited mononuclear cells were analyzed upon *T. gondii* infection (Supporting Information 2A-H'). Here no differences were observed in MFI values or cells positively producing these proteins. To address the question whether the altered cytokine milieu in infected brains of p75^{-/-} mice would affect the survival of cells, we performed an apoptosis assay via flow cytometry (Supporting Information 3A, B). While the frequencies of living cells and apoptotic cells did not differ between WT and p75^{-/-} animals, necrotic cells were significantly reduced in KO mice ($p < .03$).

In summary, we found that knockout of p75^{NTR} leads to a higher secretion of proinflammatory mediators and anti-inflammatory IL-10 by myeloid cell populations but had no effect on brain resident microglia.

3.5 | Chronic infection with *T. gondii* increases proBDNF levels in WT and p75^{-/-} mice

Previously, we reported that infection with *T. gondii* induces changes in the morphology of noninfected neurons and also leads to modified brain connectivity in rodents (Parlog et al., 2014) possibly explaining the behavioral changes observed in infected rats (Berday, Webster, & Macdonald, 2000). With regards to this, related studies have reported a link between changes in neurotrophin levels and the progression of neurodegenerative diseases such as schizophrenia and Alzheimer's disease (Capsoni, Brandi, Arisi, D'Onofrio, & Cattaneo, 2011; Green, Matheson, Shepherd, Weickert, & Carr, 2011). To obtain more information about possible changes in neurotrophin expression levels within the CNS of WT and p75^{-/-} mice upon the infection with *T. gondii* we performed Western blot analysis. Isolated proteins from brain lysate of noninfected and infected WT and p75^{-/-} mice were analyzed for NGF, BDNF, and proBDNF levels (Figure 8a-d). Neither infection with *T. gondii* nor knockout of p75^{NTR} was found to have an effect on NGF or BDNF levels which remained at baseline (NGF: WT control vs. WT inf.: $p < .99$; p75^{-/-} control vs. p75^{-/-} inf.: $p < .74$ / BDNF: WT control vs. WT inf.: $p < .75$; p75^{-/-} control vs. p75^{-/-} inf.: $p < .99$; Figure 8b, c). Remarkably, proBDNF which was detectable in small quantities in control WT and p75^{-/-} mice increased strongly upon *T. gondii* infection (WT control vs. WT inf.: $p < .0001$; p75^{-/-} control vs. p75^{-/-} inf.: $p < .0001$; Figure 8d). Assuming that this observed upregulation of proBDNF was possibly facilitated by the recruited immune cell populations due to *T. gondii* infection, we set out to confirm our hypothesis. To this end, peripheral immune cells were isolated from spleens of control and infected WT mice and proBDNF expression was analyzed by Western blot (Figure 8e, f). While protein levels of the proneurotrophin were detectable at lower

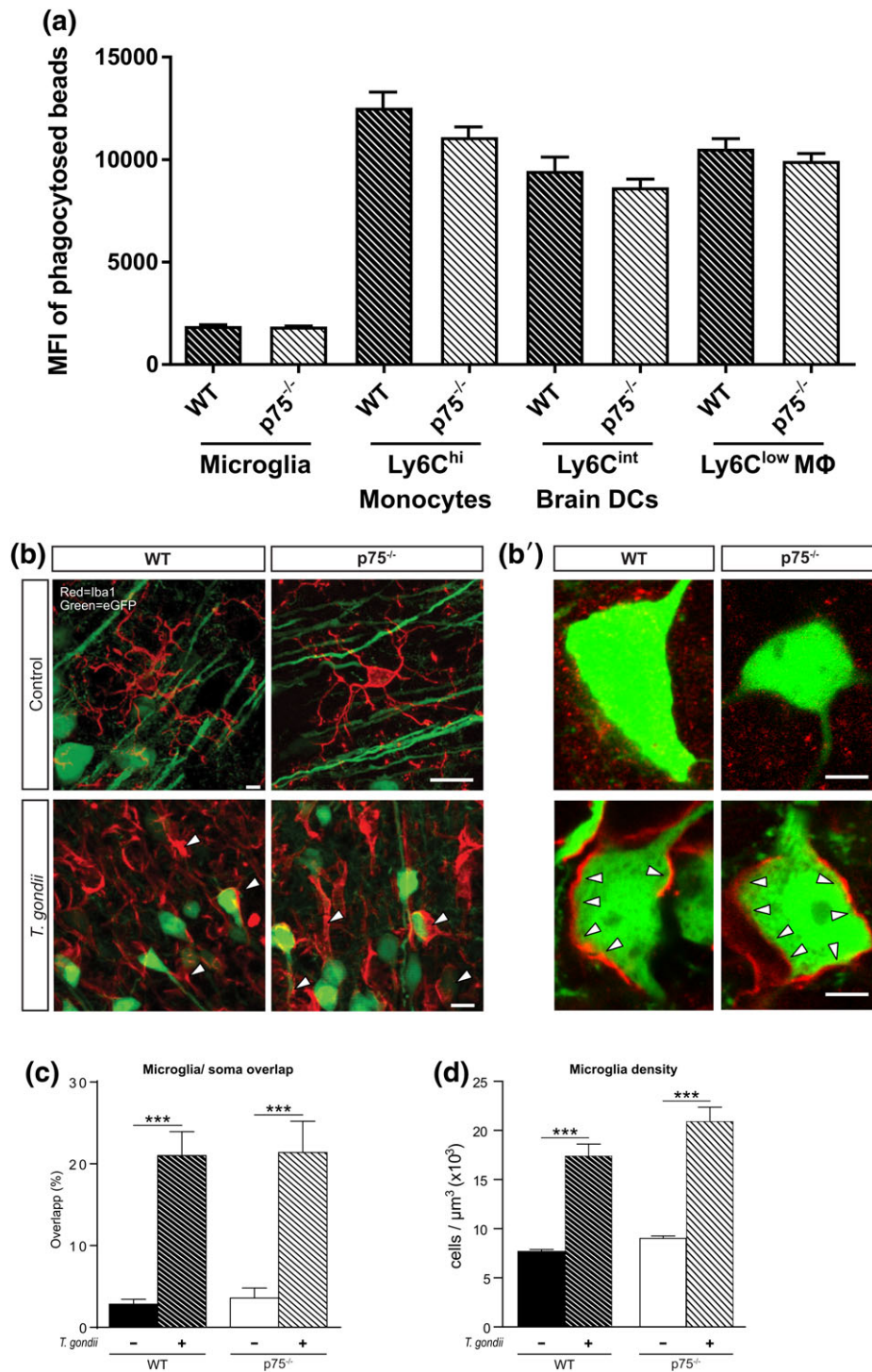


FIGURE 5 Ex vivo phagocytosis assay of immune cells isolated from brains of WT and p75^{-/-} mice infected with *T. gondii*. (a) The phagocytic capability of immune cells isolated from *T. gondii*-infected brains of WT and p75^{-/-} mice was assessed ex vivo by a phagocytosis assay. Isolated cells were incubated together with FITC-fluorescent latex beads and analyzed by flow cytometry. Cell populations were selected as described above and Bar charts display the MFI (\pm SEM) in the FITC detection channel. Differences between groups were analyzed by Mann-Whitney test. (b) The images above show a typical resting Iba1⁺ microglia (red) under control conditions for hippocampal CA1 region of WT (left) and p75^{-/-} mice (right). Below are typical images of activated Iba1⁺ microglia (red) upon chronic *T. gondii* infection for hippocampal CA1 region of WT (left) and p75^{-/-} mice (right). In green are eGFP-labeled CA1 pyramidal neurons. Scale bars are 50 μ m. (b') The images show a higher magnification (scale bar is 10 μ m) of eGFP⁺ CA1 pyramidal cell bodies and Iba1⁺ microglia processes under control conditions (above) and chronic *T. gondii* infection (below) for WT (left) and p75^{-/-} mice (right). (c) Bar charts show the quantification for the overlay (in %) between Iba1⁺ microglia processes and eGFP⁺ cell bodies for WT and p75^{-/-} mice under control conditions and upon chronic *T. gondii* infection. (d) Bar charts show the quantification for Iba1⁺ microglia density for WT and p75^{-/-} mice under control conditions and chronic *T. gondii* infection. Differences between groups were analyzed by Student's *T*-test. All values are shown as mean \pm SEM (***) $p < .001$

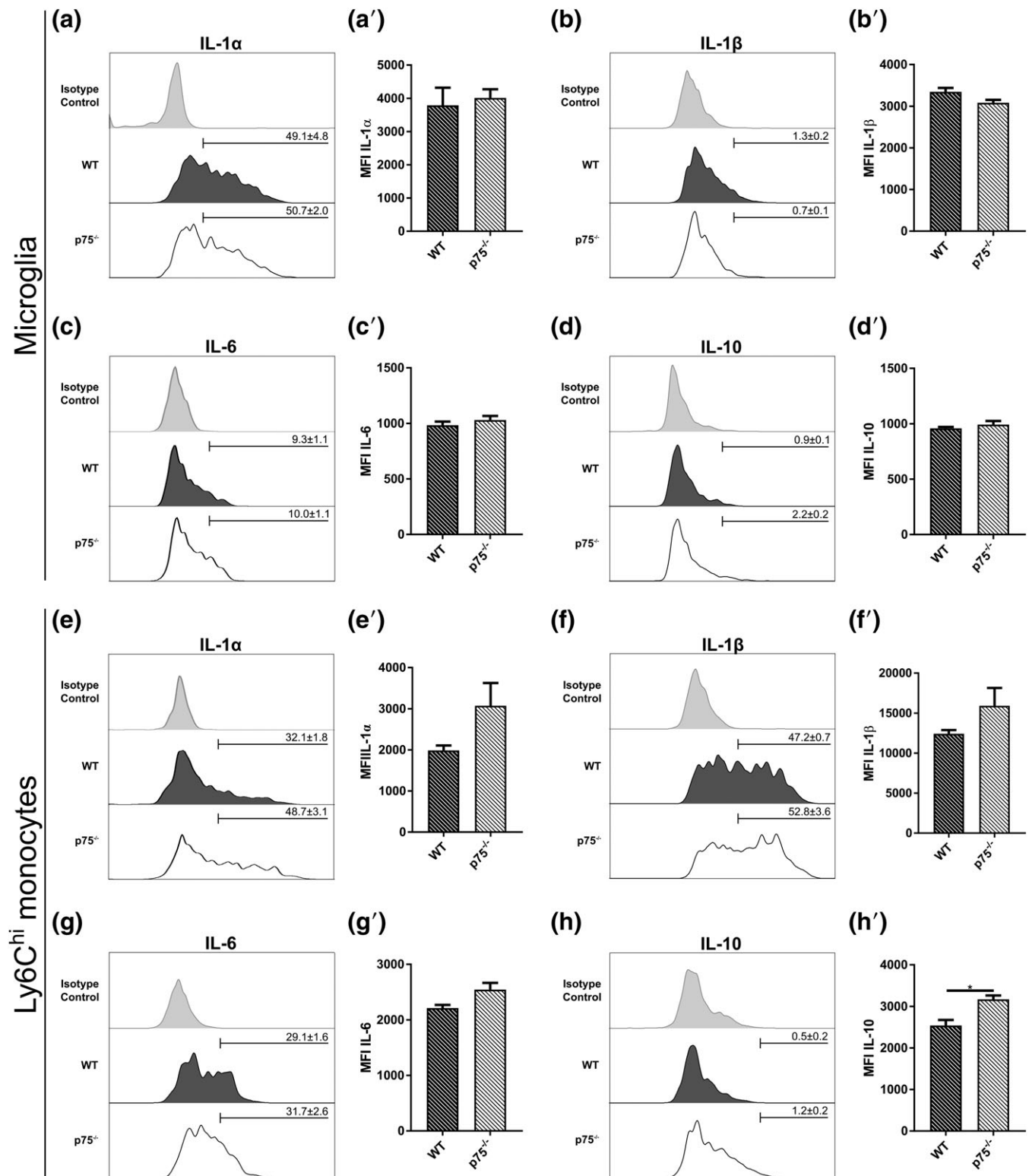


FIGURE 6 Flow cytometric analysis of intracellular cytokines in microglia and Ly6C^{hi} monocytes from brains of *T. gondii*-infected WT and p75^{-/-} mice. Isolated cells from brains of *T. gondii*-infected WT and p75^{-/-} mice were re-stimulated with *Toxoplasma* lysate antigen in vitro and intracellular proteins were stained for flow cytometric analysis. Cell populations were selected as described above. (a–h) Histograms show the representative intracellular expression level of the molecules by cells (WT mice tinted, p75^{-/-} mice without tint) in comparison to the corresponding isotype control. Bars mark cells positive for the particular protein and numbers above bars show the percentage of cells (\pm SEM) in the respective population. (a'–h') Bar charts display the MFI (\pm SEM) for the respective fluorochrome-conjugated antibody for the particular protein. Differences between groups were analyzed by Mann-Whitney test (* $p < .05$)

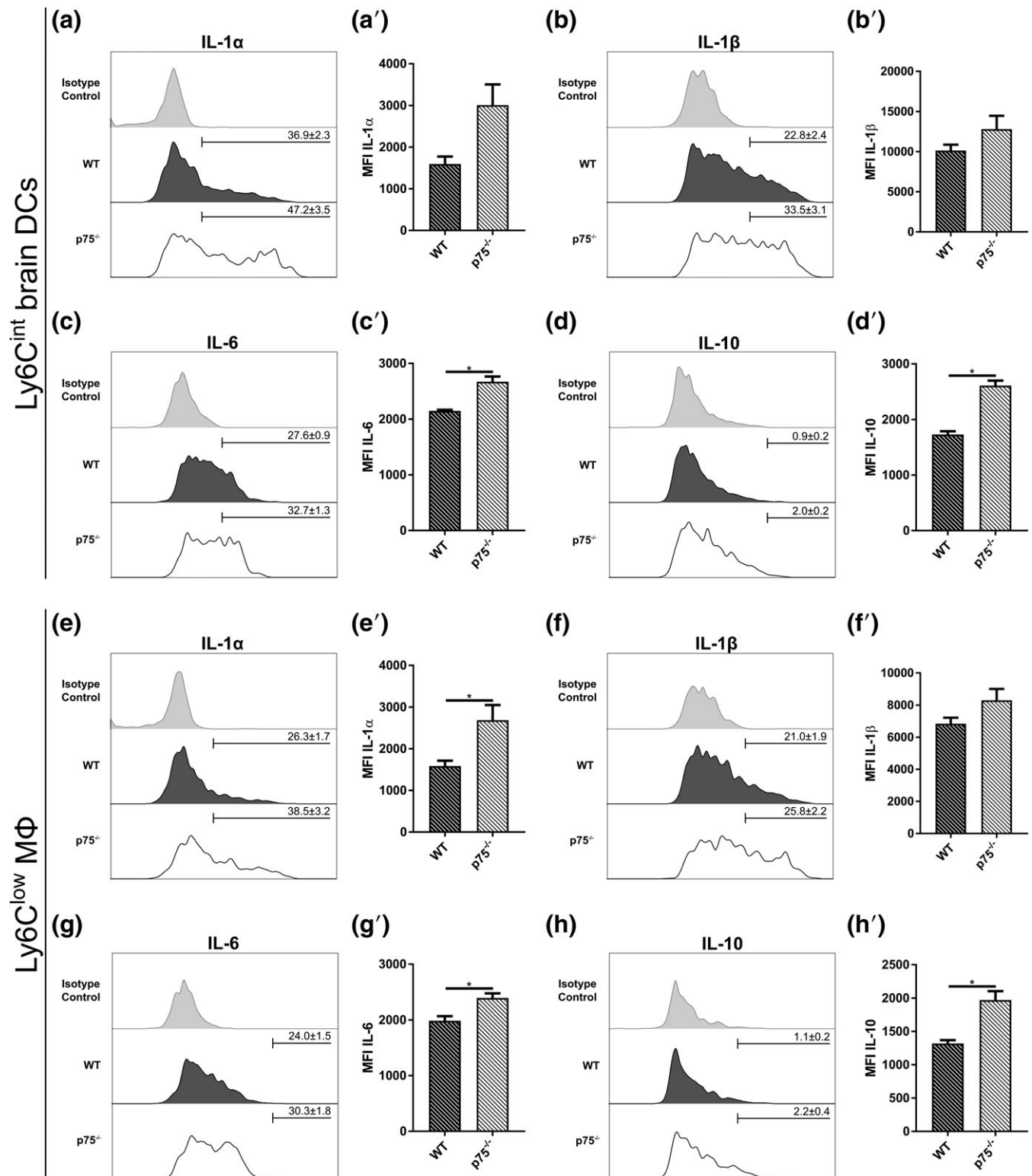


FIGURE 7 Flow cytometric analysis of intracellular cytokines in Ly6C^{int} brain DCs and Ly6C^{low} macrophages from brains of *T. gondii*-infected WT and p75^{-/-} mice. Isolated cells from brains of *T. gondii*-infected WT and p75^{-/-} mice were re-stimulated with *Toxoplasma* lysate antigen in vitro and intracellular proteins were stained for flow cytometric analysis. Cell populations were selected as described above. (a–h) Histograms show the representative intracellular expression level of the molecules by cells (WT mice tinted, p75^{-/-} mice without tint) in comparison to the corresponding isotype control. Bars mark cells positive for the particular protein and numbers above bars show the percentage of cells (±SEM) in the respective population. (a'–h') Bar charts display the MFI (±SEM) for the respective fluorochrome-conjugated antibody for the particular protein. Differences between groups were analyzed by Mann-Whitney test (**p* < .05)

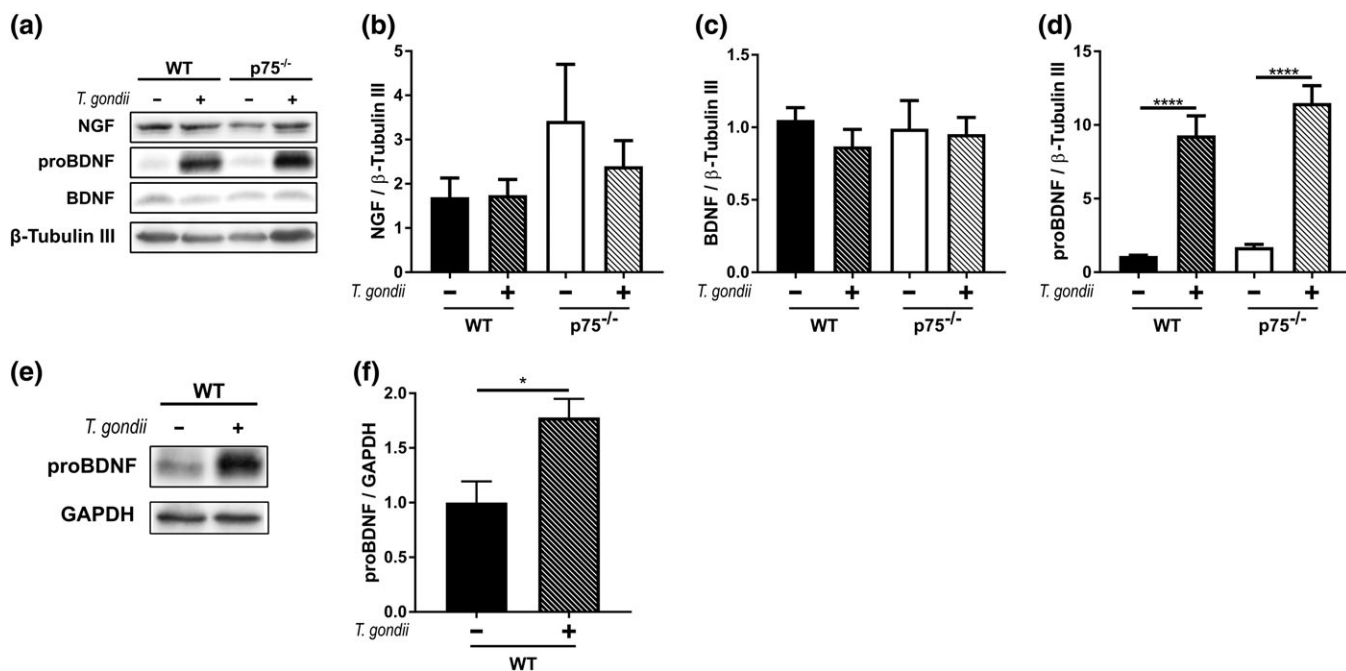


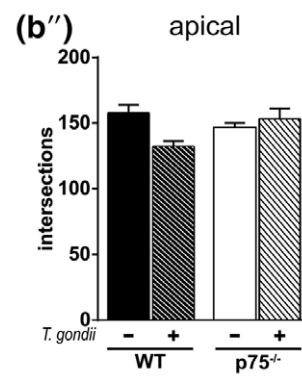
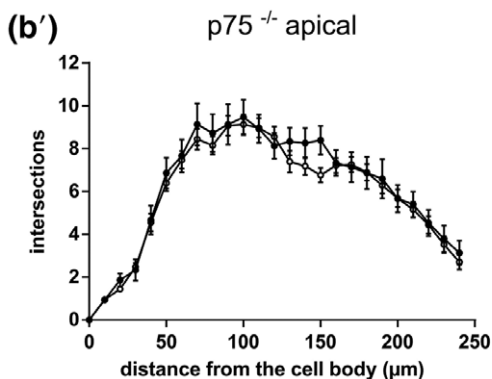
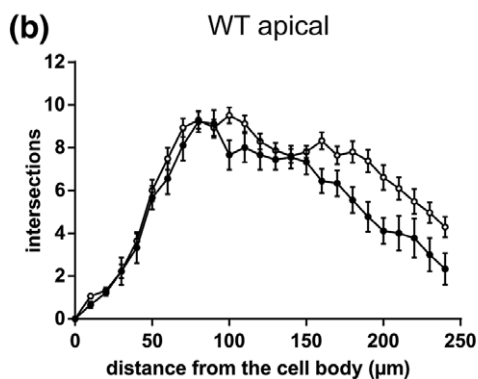
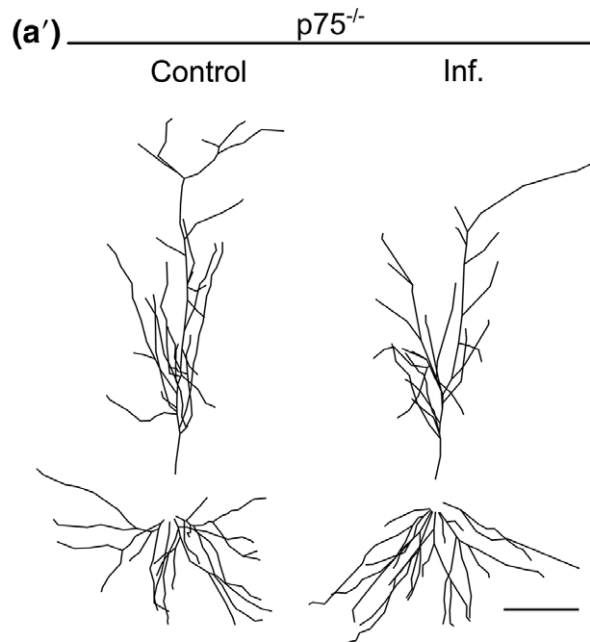
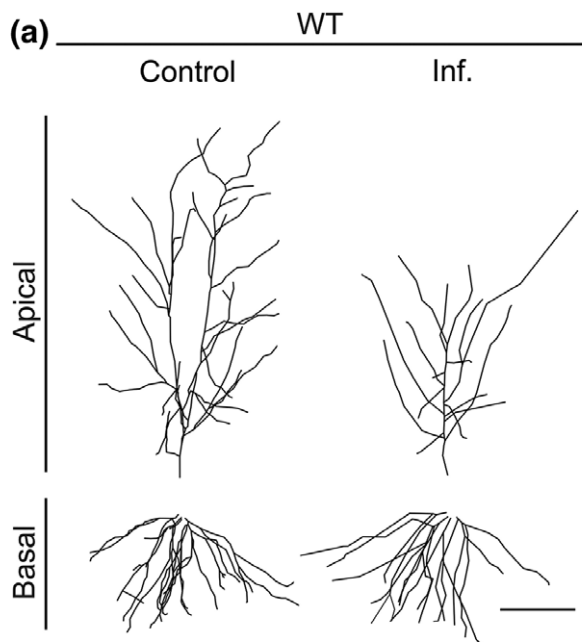
FIGURE 8 Western blot analysis of neurotrophins protein levels in brains of *T. gondii*-infected WT and p75^{-/-} mice and from isolated immune cells. (a–d) Western blot analysis of NGF, BDNF and proBDNF in whole-brain lysate from control and infected mice, alongside β -Tubulin-III loading controls. Bar charts indicate densitometric analysis of blots, expressed as mean (\pm SEM). Differences between groups were analyzed using a one-way ANOVA with post-hoc Tukey's HSD test. (e, f) Western blot analysis of proBDNF in isolated immune cells from control and *T. gondii*-infected WT mice with GAPDH loading controls. Bar charts indicate densitometric analysis of blots, expressed as mean (\pm SEM). Differences between groups were analyzed by Mann-Whitney test. (* $p < 0.05$, **** $p < 0.0001$)

quantities in control mice, *T. gondii* infection significantly increased the levels of proBDNF (WT control vs. WT inf.: $p < .03$) supporting our previous findings in brain homogenate. Taken together we could show that protein levels of NGF and BDNF were neither affected by p75^{NTR} KO nor by *T. gondii* infection. In contrast, proBDNF levels were found highly increased in the brain and periphery of infected mice.

3.6 | Role of p75^{NTR} in mediating the effect of a chronic *T. gondii* infection on dendritic architecture

Chronic infection with *T. gondii* was shown to result in a significant reduction in neuronal morphology and connectivity both in the cortex and hippocampus of C57BL/6 mice (Parlog et al., 2014). Interestingly, the p75^{NTR} was reported to specifically mediate negative structural changes at pyramidal neurons (Zagrebelsky et al., 2005) and its expression levels are modulated upon neuroinflammation (Meeker & Williams, 2014). Thus, we addressed whether knocking out p75^{NTR} might rescue neuronal morphology upon *T. gondii* infection. While at a qualitative level dendritic complexity of CA1 pyramidal neurons is clearly reduced in WT mice upon chronic *T. gondii* infection (Figure 9a), no obvious differences in dendritic architecture can be observed in infected p75^{-/-} mice (Figure 9a'). Further, Sholl analysis was applied to quantify dendritic complexity relative to the distance from the cell body. When comparing control (open circles) and infected WT mice (black circles) a significantly lower dendritic complexity along the entire length of both the apical (Figure 9b; $F(1,38) = 4.677$ $p < .05$) but not the basal (Figure 9c) dendritic trees

was detected upon *T. gondii* infection. When p75^{-/-} mice were analyzed no significant difference in dendritic complexity could be observed along the entire length of the apical dendrite (Figure 9b') upon *T. gondii* infection (black circles) compared to noninfected p75^{-/-} mice (open circles). On the contrary, dendritic complexity for the basal dendrites of CA1 pyramidal neurons of p75^{-/-} mice was significantly lower in the proximal part (Figure 9c'; $F(1, 52) = 4.283$ $p < .05$) during infection (black circles). The analysis of total dendritic complexity confirmed the observations above and showed a slight decrease in WT mice upon *T. gondii* infection for the apical but not for the basal dendrites (Figure 9b'', c''; Table 1). Interestingly, total dendritic complexity was not significantly decreased for both apical and basal dendrites of infected p75^{-/-} mice when compared to controls (Figure 9b'', c''; Table 1). Taken together these results confirm previous findings showing a significant loss in neuronal complexity in WT mice upon *T. gondii* infection and indicate that deletion of p75^{NTR} prevents the *T. gondii*-induced changes in dendritic architecture of CA1 pyramidal neurons. Next, we compared dendritic spine density changes in WT and p75^{-/-} cortical and hippocampal pyramidal neurons upon *T. gondii* infection. Both for CA1 and for Layer V/VI pyramidal neurons, dendritic spine density was significantly reduced during infection in WT mice (Figure 9d–e'; CA1 apical dendrites $p < .05$; CA1 basal $p < .01$; LV/VI apical $p < .01$; LV/VI basal $p < .001$). In p75^{-/-} mice, dendritic spine density upon *T. gondii* infection was only slightly, but not significantly lower than in noninfected mice for both compartments of CA1 pyramidal neurons and for the basal dendrites of Layer V/VI pyramidal neurons (Figure 9d–e'; Table 1). The only exceptions were the LV/VI apical dendrites showing a significantly lower spine



○ Control ● Inf.

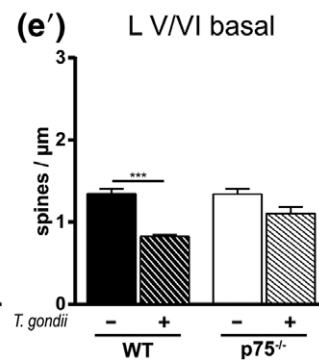
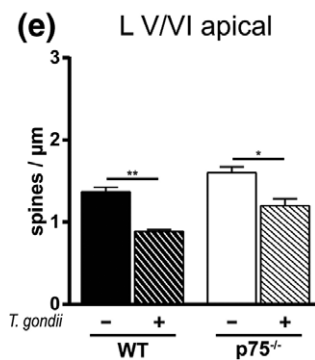
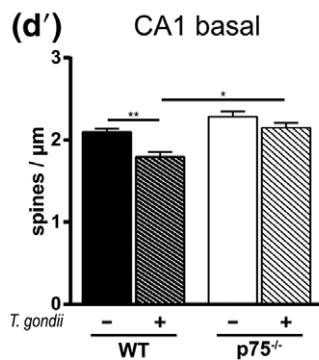
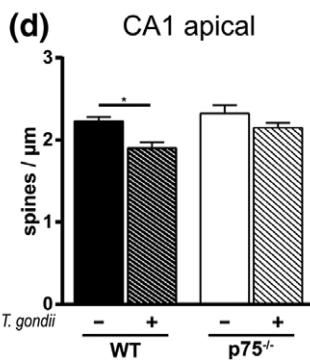
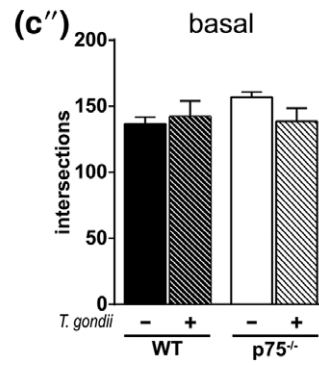
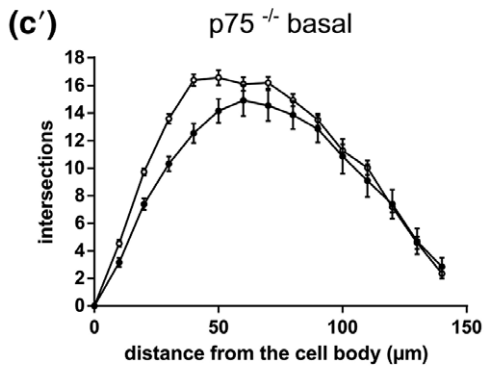
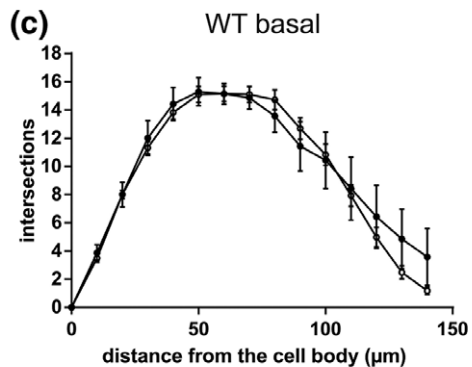


FIGURE 9 Role of p75^{NTR} in mediating the effect of a *T. gondii* infection on dendritic architecture. (a, a') Typical camera lucida reconstructions for the apical and basal dendrites of WT and p75^{-/-} CA1 pyramidal neurons under control conditions and of infected mice with *T. gondii*. Scale bars are 100 μ m. (b, b') The graphs show the Sholl analysis for the apical dendrites of CA1 hippocampal pyramidal neurons of WT and p75^{-/-} CA1 pyramidal neurons under control conditions (open circles) and upon *T. gondii* infection (black circles). (b'') The graph shows total dendritic complexity for the apical dendrites of CA1 hippocampal pyramidal neurons of WT and p75^{-/-} CA1 pyramidal neurons under control conditions and upon *T. gondii* infection. (c, c') The graphs show the Sholl analysis for the basal dendrites of CA1 hippocampal pyramidal neurons of WT and p75^{-/-} CA1 pyramidal neurons under control conditions (open circles) and upon *T. gondii* infection (black circles). (c'') The graph shows total dendritic complexity for the basal dendrites of CA1 hippocampal pyramidal neurons of WT and p75^{-/-} CA1 pyramidal neurons under control conditions and upon *T. gondii* infection. (d, d') The graphs show dendritic spine density for the apical and basal dendrites of WT and p75^{-/-} CA1 pyramidal neurons under control conditions and upon *T. gondii* infection. (e, e') The graphs show dendritic spine density for the apical and basal dendrites of WT and p75^{-/-} layer V/VI pyramidal neurons under control conditions and upon *T. gondii* infection. Total complexity and spine density were compared between groups using a one-way ANOVA with post hoc Tukey's HSD test. All values are shown as mean \pm SEM (* $p < .05$; ** $p < .01$; *** $p < .001$)

density than controls upon infection (Figure 9e; $p < .05$). For the CA1 basal dendrites dendritic spine density was significantly higher for infected p75^{-/-} mice versus infected WT mice (Figure 9d'; Table 1; CA1 basal $p < .05$). Thus, deletion of p75^{NTR} results in a complete rescue of the decrease in dendritic spine density induced by *T. gondii* infection for the CA1 pyramidal neurons and a partial one for Layer V/VI pyramidal neurons.

4 | DISCUSSION

We recently detected significant alterations in dendritic complexity and dendritic spine density in CNS principal neurons upon cerebral toxoplasmosis (Parlog et al., 2014). In addition, Western blot analysis revealed decreased levels of the presynaptic protein Synatophysin

and the postsynaptic protein PSD-95 indicating a significant modification of brain connectivity upon *T. gondii* infection (Parlog et al., 2014). Moreover, our results indicate distinct modifications in the synaptic protein composition (Lang et al., 2018). We previously reported that the chronic infection causes activation of resident microglia and recruitment of mononuclear immune cell subsets to the CNS (Biswas et al., 2015, 2017; Möhle et al., 2016). Thus, we hypothesized that activated immune cells possibly interact with neurons upon infection and modify their morphology and function. However, the molecular and cellular mechanisms mediating such interaction remained unexplored (Parlog et al., 2015). Neurotrophin signaling has been shown to modulate the immune system activity at different levels (Minnone, de Benedetti, & Bracci-Laudiero, 2017; Vega et al., 2003). Therefore, we investigated the role of p75^{NTR} signaling in modulating neuronal architecture and immune cell function in the CNS. We showed that p75^{NTR} influences immune cell activation, function, and cytokine production possibly contributing to the rescue of neuronal structure. Moreover, we revealed that infection-induced decrease in dendritic complexity observed upon *T. gondii* infection could be rescued by p75^{NTR} knockout.

In addition to neurons, the expression of p75^{NTR} was also detected on a variety of immune cells such as B cells and peripheral mononuclear blood cells (Morgan, Thorpe, Marchetti, & Perez-Polo, 1989). Based on those previous observations, we aimed at investigating whether p75^{NTR} expression is altered on peripheral blood mononuclear cell subsets during *T. gondii* infection. Our results already showed a prominent expression of p75^{NTR} on mononuclear cells in the blood of control mice under steady state conditions. Infection with *T. gondii* led to an increased receptor expression that was found on Ly6C^{hi} inflammatory monocytes and Ly6C^{low} resident macrophages. These results are in line with results by Choi and Friedman (2009) who reported an increase of p75^{NTR} expression in astrocytes and neurons as a response to high levels of IL-1 β and TNF. Noteworthy, these cytokines have also been shown to be important mediators in the course of *T. gondii* infection (Chang, Grau, & Pechère, 1990; Dimier & Bout, 1993; Schlüter et al., 1999; Yap, Schariton-Kersten, Charest, & Sher, 1998).

Next, we examined p75^{NTR} expression by resident and recruited immune cells in the CNS upon infection-induced neuroinflammation. While lymphocytes did not express this receptor, resident microglia cells and myeloid-derived mononuclear cell subsets upregulated p75^{NTR}. Importantly, Ly6C^{low} macrophages revealed the most

TABLE 1 Statistical values for total dendritic spine density in different brain areas and different neuronal subregions

Values for total dendritic complexity (Figure 9b',c''; apical)		
Mice	Control	<i>T. gondii</i> infection
WT	31; 157.7 \pm 6.21	9; 132.1 \pm 4.20
p75 ^{-/-}	38; 146.1 \pm 4.07	15; 153.3 \pm 7.79
Values for total dendritic complexity (Figure 9b',c''; basal)		
Mice	Control	<i>T. gondii</i> infection
WT	29; 136.8 \pm 5.06	7; 142.3 \pm 11.70
p75 ^{-/-}	41; 156.9 \pm 3.86	13; 138.5 \pm 10.13
Values for total dendritic spine density apical CA1 (Figure 9d)		
Mice	Control	<i>T. gondii</i> infection
WT	14; 2.23 \pm 0.05	3; 1.90 \pm 0.07
p75 ^{-/-}	5; 2.32 \pm 0.09	4; 2.15 \pm 0.05
Values for total dendritic spine density basal CA1 (Figure 9d')		
Mice	Control	<i>T. gondii</i> infection
WT	12; 2.09 \pm 0.04	3; 1.79 \pm 0.05
p75 ^{-/-}	5; 2.28 \pm 0.06	4; 2.07 \pm 0.06
Values for total dendritic spine density apical L V/VI (Figure 9e)		
Mice	Control	<i>T. gondii</i> infection
WT	14; 1.36 \pm 0.05	3; 0.88 \pm 0.02
p75 ^{-/-}	5; 1.60 \pm 0.03	4; 1.19 \pm 0.08
Values for total dendritic spine density basal L V/VI (Figure 9e')		
Mice	Control	<i>T. gondii</i> infection
WT	13; 1.34 \pm 0.05	3; 0.82 \pm 0.01
p75 ^{-/-}	5; 1.34 \pm 0.06	4; 1.10 \pm 0.07



prominent upregulation of p75^{NTR} suggesting a potential effect on their function.

Previously we have described the crucial involvement of recruited peripheral myeloid cells in host defense against *T. gondii* infection (Dunay et al., 2008). In the murine model of cerebral toxoplasmosis we found that Ly6C^{hi} inflammatory monocytes were recruited from the blood to the brain in a CCL2-dependent manner to exert anti-parasitic activities (Biswas et al., 2015). First, recruited Ly6C^{hi} inflammatory monocytes produced proinflammatory mediators such as IL-1 α , IL-6, and inducible nitric oxide synthase (iNOS) but were also able to secrete regulatory IL-10. Second, Ly6C^{hi} inflammatory monocytes further differentiated into Ly6C^{int} brain DCs and Ly6C^{low} macrophages upon arrival in the CNS and, thus, contributed to antigen presentation and to parasite control.

Due to the high p75^{NTR} expression on Ly6C^{hi} inflammatory monocytes in the blood, we investigated whether knockout of p75^{NTR} would affect the recruitment of monocytes to the CNS upon *T. gondii* infection. Previous in vitro studies have reported beneficial effects of NGF-associated neurotrophin signaling on macrophage chemotaxis (Kobayashi & Mizisin, 2001; Samah et al., 2008) but in contrast, animal models of experimental autoimmune encephalomyelitis demonstrated a reduced CNS infiltration of blood monocytes caused by NGF overexpression (Flügel et al., 2001). Here, we did not detect significant differences in the frequencies of myeloid cells in cortex or hippocampus of p75^{-/-} mice. Furthermore, the in vitro migratory response of leukocytes towards CCL2 stimulation was not changed. The observed differences can possibly be explained by the difference in the model of neuroinflammation and by the circumstance that NGF protein levels were not affected by KO of p75^{NTR}. Recent findings by Lee et al. (2016) reported reduction in CNS trafficking of inflammatory monocytes after applying a p75^{NTR} blocking antagonist. However, this study only tested the effects of the p75^{NTR} antagonist on other members of the TNF receptor family with cysteine-rich domains. Thus, they did not exclude interactions of this antagonist with other extracellular receptors which may be an explanation for the altered cell recruitment and activation (Delbary-Gossart et al., 2016).

Early studies revealed that neurotrophin signaling affects several functions of immune cells such as inhibition of MHC class II expression, phagocytosis and proliferation (Elkabes, DiCicco-Bloom, & Black, 1996; Neumann, Misgeld, Matsumuro, & Wekerle, 1998). As the immune cell activation status reflects their functional properties, we characterized the phenotype of immune cells in the brains of p75^{-/-} mice upon *Toxoplasma*-induced neuroinflammation. Here, we found that brain resident microglia and subsets of recruited peripheral myeloid cells in knockout mice displayed lower levels of MHC class II, CD11c, F4/80, and CD80 surface receptors implying an altered activation and function. Therefore, we analyzed the phagocytic capacity of these immune cells but did not find differences when compared to WT animals. Besides phagocytosis, the production of inflammatory mediators is another functional aspect of the cellular immune response toward inflammation. Accordingly, we analyzed cytokine production by microglia and recruited peripheral mononuclear cell subsets. Although p75^{NTR} knockout did not affect microglia cells, myeloid cell subsets secreted increased amounts of proinflammatory IL-1 α , IL-6, and regulatory IL-10. So far, few studies have reported

about the effects of neurotrophins on the release of immunological mediators by immune cells and even less is known about the role of the p75^{NTR} in this context. (Barouch et al., 2001) observed the secretion of nitric oxide by macrophages in an NGF-dependent activation of mitogen-activated protein kinases. In our experiments, we did not find alterations in the production of iNOS suggesting that the reported nitric oxide release could be rather a result of TrkA- instead of p75^{NTR}-mediated signal transduction (Frossard, Freund, & Advenier, 2004; Stephens et al., 1994; Xie, Tisi, Yeo, & Longo, 2000).

The proinflammatory cytokine IL-1 was shown in many studies to be involved in memory processes, specifically those related to hippocampal functioning (Goshen & Yirmiya, 2007). Although most of the evidence gathered so far indicates that the effects of IL-1 on CNS neurons are detrimental, recent evidence suggests that under some circumstances IL-1 may actually be required for the normal physiological regulation of hippocampal function (Avital et al., 2003). Indeed, impairment of IL-1 signaling results in a reduced size of dendritic spines on hippocampal pyramidal neurons (Goshen & Yirmiya, 2009). Also, application of IL-10 to hippocampal neurons has been shown to induce synapse formation (Lim et al., 2013). Taken together, the increase we observed in the secretion of IL-1 α and IL-10 in p75^{-/-} mice might at least in part contribute to the rescuing of neuronal structure upon *T. gondii* infection.

The multifunctional cytokine IL-6 was reported to be a promotor and inhibitor of inflammation (Scheller, Chalaris, Schmidt-Arras, & Rose-John, 2011; Tilg, Dinarello, & Mier, 1997; Xing et al., 1998) and has been associated with a variety of neurodegenerative disorders including Alzheimer's and Parkinson disease (Dobbs et al., 1999; Wood et al., 1993). IL-6 was also found to induce neuroprotection and prevent neuron and oligodendrocyte degradation (Chucair-Elliott et al., 2014; Pizzi et al., 2004), thus contributing to its multifunctional aspects. Accordingly, our data showed an increased secretion of IL-6 by Ly6C^{int} brain DCs and Ly6C^{low} macrophages, supporting these previous findings.

BDNF signaling has been shown to positively modulate dendritic and spine architecture in cortical and hippocampal neurons as well as structural plasticity both in vitro and in vivo (Kellner et al., 2014; Rauskolb et al., 2010; Zagrebelsky & Korte, 2014). We performed Western blot analysis of brain homogenates to compare BDNF protein levels. Here, we found that BDNF levels remained unaltered upon infection for both WT and p75^{-/-} mice. Interestingly, the precursor protein proBDNF was strongly increased upon infection. Particularly, signaling of proBDNF via the p75^{NTR} has been shown to promote spine pruning and to negatively affect dendritic spine density and synaptic plasticity (Orefice, Shih, Xu, Waterhouse, & Xu, 2016; Qiao, An, Xu, & Ma, 2017; Yang et al., 2014). In addition, our data imply that activated immune cells contribute to proBDNF production upon infection-induced inflammation since previous studies also observed the secretion of proBDNF by peripheral macrophages under certain inflammatory conditions (Luo et al., 2016; Wong et al., 2010). Thus, activated resident or recruited immune cells entering the CNS from the periphery during neuroinflammation possibly contribute to the elevated proBDNF levels in the CNS. Our results suggest that the rescue of the *Toxoplasma* infection-induced alterations of neuronal architecture observed in p75^{-/-} animals may be due to the absence of

proBDNF-mediated signaling in neurons in combination with the altered immune response. Yet, it is not clear whether other cell types are also involved in this observed rescue of neuronal morphology. A study published by Cragolini, Huang, Gokina, and Friedman (2009) demonstrated that astrocytes are capable of expressing p75^{NTR} upon seizures. Unfortunately, this study only addressed the impact of NGF on p75^{NTR} signaling, leaving the effect of proneurotrophins on astrocyte activation unraveled. Accordingly, as for mature neurotrophins, only little is known about the final role of proneurotrophins in immune cell activation. Of note, two studies conducted on peripheral macrophages pointed out that proneurotrophins are able to alter the migratory behavior and phenotype of these cells (Williams, Killebrew, Clary, Seawell, & Meeker, 2015; Wong et al., 2010). Although the altered phenotype of immune cells in p75^{-/-} mice could be caused by the lack of proneurotrophin signaling, it remains unclear why cytokine expression was different in recruited myeloid cells but not in microglia. In addition, the question arises whether the high levels of proBDNF in infected peripheral immune cells can also mediate the activation of myeloid cells before entering the CNS. To this end, further experiments need to be carried out addressing the effect of mature neurotrophins and their precursor forms on immune cell activation in the brain and periphery during steady state and upon inflammatory conditions.

Taken together, our data provide evidence that neurotrophin signaling via the p75^{NTR} alters innate immune cell behavior and contributes to function and structural rearrangements in the neuronal network upon chronic *Toxoplasma* infection-induced neuroinflammation.

ACKNOWLEDGMENTS

We thank Petra Grüneberg und Dr. Abidat Schneider for their excellent technical assistance. This work was supported by the DFG (SFB854, TP25) to I.R.D. and M.K.

ORCID

Ildiko Rita Dunay  <https://orcid.org/0000-0002-9900-8605>

REFERENCES

- Avital, A., Goshen, I., Kamsler, A., Segal, M., Iverfeldt, K., Richter-Levin, G., & Yirmiya, R. (2003). Impaired interleukin-1 signaling is associated with deficits in hippocampal memory processes and neural plasticity. *Hippocampus*, 13(7), 826–834. <https://doi.org/10.1002/hipo.10135>
- Barouch, R., Kazimirsky, G., Appel, E., & Brodie, C. (2001). Nerve growth factor regulates TNF-alpha production in mouse macrophages via MAP kinase activation. *Journal of Leukocyte Biology*, 69(6), 1019–1026.
- Berdoy, M., Webster, J. P., & Macdonald, D. W. (2000). Fatal attraction in rats infected with toxoplasma gondii. *Proceedings. Biological Sciences*, 267(1452), 1591–1594. <https://doi.org/10.1098/rspb.2000.1182>
- Biswas, A., Bruder, D., Wolf, S. A., Jeron, A., Mack, M., Heimesaat, M. M., & Dunay, I. R. (2015). Ly6C(high) monocytes control cerebral toxoplasmosis. *Journal of Immunology (Baltimore, Md. : 1950)*, 194(7), 3223–3235. <https://doi.org/10.4049/jimmunol.1402037>
- Biswas, A., French, T., Düsedau, H. P., Mueller, N., Riek-Burchardt, M., Dudeck, A., ... Dunay, I. R. (2017). Behavior of neutrophil granulocytes during toxoplasma gondii infection in the central nervous system. *Frontiers in Cellular and Infection Microbiology*, 7, 259. <https://doi.org/10.3389/fcimb.2017.00259>
- Blanchard, N., Dunay, I. R., & Schlüter, D. (2015). Persistence of toxoplasma gondii in the central nervous system: A fine-tuned balance between the parasite, the brain and the immune system. *Parasite Immunology*, 37(3), 150–158. <https://doi.org/10.1111/pim.12173>
- Braun, D. J., Kalinin, S., & Feinstein, D. L. (2017). Conditional depletion of hippocampal brain-derived neurotrophic factor exacerbates neuropathology in a mouse model of Alzheimer's disease. *ASN Neuro*, 9(2), 1759091417696161. <https://doi.org/10.1177/1759091417696161>
- Capsoni, S., Brandi, R., Arisi, I., D'Onofrio, M., & Cattaneo, A. (2011). A dual mechanism linking NGF/proNGF imbalance and early inflammation to Alzheimer's disease neurodegeneration in the AD11 anti-NGF mouse model. *CNS & Neurological Disorders - Drug Targets*, 10(5), 635–647. <https://doi.org/10.2174/187152711796235032>
- Chang, H. R., Grau, G. E., & Pechère, J. C. (1990). Role of TNF and IL-1 in infections with toxoplasma gondii. *Immunology*, 69(1), 33–37.
- Chao, M. V. (2003). Neurotrophins and their receptors: A convergence point for many signalling pathways. *Nature Reviews Neuroscience*, 4(4), 299–309. <https://doi.org/10.1038/nrn1078>
- Choi, S., & Friedman, W. J. (2009). Inflammatory cytokines IL-1 β and TNF- α regulate p75NTR expression in CNS neurons and astrocytes by distinct cell-type-specific signalling mechanisms. *ASN Neuro*, 1(2), AN20090009. <https://doi.org/10.1042/AN20090009>
- Chucair-Elliott, A. J., Conrady, C., Zheng, M., Kroll, C. M., Lane, T. E., & Carr, D. J. J. (2014). Microglia-induced IL-6 protects against neuronal loss following HSV-1 infection of neural progenitor cells. *Glia*, 62(9), 1418–1434. <https://doi.org/10.1002/glia.22689>
- Cragolini, A. B., Huang, Y., Gokina, P., & Friedman, W. J. (2009). Nerve growth factor attenuates proliferation of astrocytes via the p75 neurotrophin receptor. *Glia*, 57(13), 1386–1392. <https://doi.org/10.1002/glia.20857>
- Delbary-Gossart, S., Lee, S., Baroni, M., Lamarche, I., Arnone, M., Canolle, B., ... Beattie, M. S. (2016). A novel inhibitor of p75-neurotrophin receptor improves functional outcomes in two models of traumatic brain injury. *Brain: A Journal of Neurology*, 139(Pt 6), 1762–1782. <https://doi.org/10.1093/brain/aww074>
- Dimier, I. H., & Bout, D. T. (1993). Co-operation of interleukin-1 beta and tumour necrosis factor-alpha in the activation of human umbilical vein endothelial cells to inhibit toxoplasma gondii replication. *Immunology*, 79(2), 336–338.
- Dobbs, R. J., Charlett, A., Purkiss, A. G., Dobbs, S. M., Weller, C., & Peterson, D. W. (1999). Association of circulating TNF- α and IL-6 with ageing and parkinsonism. *Acta Neurologica Scandinavica*, 100(1), 34–41. <https://doi.org/10.1111/j.1600-0404.1999.tb00721.x>
- Dubey, J. P. (1998). Advances in the life cycle of toxoplasma gondii. *International Journal for Parasitology*, 28(7), 1019–1024. [https://doi.org/10.1016/S0020-7519\(98\)00023-X](https://doi.org/10.1016/S0020-7519(98)00023-X)
- Dunay, I. R., Damatta, R. A., Fux, B., Presti, R., Greco, S., Colonna, M., & Sibley, L. D. (2008). Gr1(+) inflammatory monocytes are required for mucosal resistance to the pathogen toxoplasma gondii. *Immunity*, 29(2), 306–317. <https://doi.org/10.1016/j.immuni.2008.05.019>
- Elkabes, S., DiCicco-Bloom, E. M., & Black, I. B. (1996). Brain microglia/macrophages express neurotrophins that selectively regulate microglial proliferation and function. *The Journal of Neuroscience*, 16(8), 2508–2521.
- Feng, G., Mellor, R. H., Bernstein, M., Keller-Peck, C., Nguyen, Q. T., Wallace, M., ... Sanes, J. R. (2000). Imaging Neuronal Subsets in Transgenic Mice Expressing Multiple Spectral Variants of GFP. *Neuron*, 28, 41–51. [https://doi.org/10.1016/S0896-6273\(00\)00084-2](https://doi.org/10.1016/S0896-6273(00)00084-2)
- Flügel, A., Matsumuro, K., Neumann, H., Klinkert, W. E. F., Birnbacher, R., Lassmann, H., ... Wekerle, H. (2001). Anti-inflammatory activity of nerve growth factor in experimental autoimmune encephalomyelitis: Inhibition of monocyte transendothelial migration. *European Journal of Immunology*, 31(1), 11–22. [https://doi.org/10.1002/1521-4141\(200101\)31:1<11::AID-IMMU11>3.0.CO;2-G](https://doi.org/10.1002/1521-4141(200101)31:1<11::AID-IMMU11>3.0.CO;2-G)
- Frossard, N., Freund, V., & Advenier, C. (2004). Nerve growth factor and its receptors in asthma and inflammation. *European Journal of Pharmacology*, 500(1–3), 453–465. <https://doi.org/10.1016/j.ejphar.2004.07.044>
- Goshen, I., & Yirmiya, R. (2007). The role of pro-inflammatory cytokines in memory processes and neural plasticity. *Psychoneuro*, 4, 337–378.



- Goshen, I., & Yirmiya, R. (2009). Interleukin-1 (IL-1): A central regulator of stress responses. *Frontiers in Neuroendocrinology*, 30(1), 30–45. <https://doi.org/10.1016/j.yfrne.2008.10.001>
- Green, M. J., Matheson, S. L., Shepherd, A., Weickert, C. S., & Carr, V. J. (2011). Brain-derived neurotrophic factor levels in schizophrenia: A systematic review with meta-analysis. *Molecular Psychiatry*, 16(9), 960–972. <https://doi.org/10.1038/mp.2010.88>
- Hashimoto, M., Nitta, A., Fukumitsu, H., Nomoto, H., Shen, L., & Furukawa, S. (2005). Involvement of glial cell line-derived neurotrophic factor in activation processes of rodent macrophages. *Journal of Neuroscience Research*, 79(4), 476–487. <https://doi.org/10.1002/jnr.20368>
- Hermes, G., Ajioka, J. W., Kelly, K. A., Mui, E., Roberts, F., Kasza, K., ... McLeod, R. (2008). Neurological and behavioral abnormalities, ventricular dilatation, altered cellular functions, inflammation, and neuronal injury in brains of mice due to common, persistent, parasitic infection. *Journal of Neuroinflammation*, 5, 48. <https://doi.org/10.1186/1742-2094-5-48>
- Hill, D. E., Chirukandoth, S., & Dubey, J. P. (2005). Biology and epidemiology of toxoplasma gondii in man and animals. *Animal Health Research Reviews*, 6(01), 41–61. <https://doi.org/10.1079/AHR2005100>
- Ibáñez, C. F., & Simi, A. (2012). p75 neurotrophin receptor signaling in nervous system injury and degeneration: Paradox and opportunity. *Trends in Neurosciences*, 35(7), 431–440. <https://doi.org/10.1016/j.tins.2012.03.007>
- Kaplan, D. R., & Miller, F. D. (2000). Neurotrophin signal transduction in the nervous system. *Current Opinion in Neurobiology*, 10(3), 381–391. [https://doi.org/10.1016/S0959-4388\(00\)00092-1](https://doi.org/10.1016/S0959-4388(00)00092-1)
- Kellner, Y., Gödecke, N., Dierkes, T., Thieme, N., Zagrebelsky, M., & Korte, M. (2014). The BDNF effects on dendritic spines of mature hippocampal neurons depend on neuronal activity. *Frontiers in Synaptic Neuroscience*, 6, 5. <https://doi.org/10.3389/fnsyn.2014.00005>
- Kobayashi, H., & Mizisin, A. P. (2001). Nerve growth factor and neurotrophin-3 promote chemotaxis of mouse macrophages in vitro. *Neuroscience Letters*, 305(3), 157–160. [https://doi.org/10.1016/S0304-3940\(01\)01854-7](https://doi.org/10.1016/S0304-3940(01)01854-7)
- Kruse, N., Cetin, S., Chan, A., Gold, R., & Lühder, F. (2007). Differential expression of BDNF mRNA splice variants in mouse brain and immune cells. *Journal of Neuroimmunology*, 182(1–2), 13–21. <https://doi.org/10.1016/j.jneuroim.2006.09.001>
- Lang, D., Schott, B. H., van Ham, M., Morton, L., Kulikovskaja, L., Herrera-Molina, R., ... Dunay, I. R. (2018). Chronic toxoplasma infection is associated with distinct alterations in the synaptic protein composition. *Journal of Neuroinflammation*, 15(1), 438. <https://doi.org/10.1186/s12974-018-1242-1>
- Lee, R., Kermani, P., Teng, K. K., & Hempstead, B. L. (2001). Regulation of cell survival by secreted proneurotrophins. *Science*, 294(5548), 1945–1948. <https://doi.org/10.1126/science.1065057>
- Lee, S., Mattingly, A., Lin, A., Sacramento, J., Mannent, L., Castel, M.-N., ... Beattie, M. S. (2016). A novel antagonist of p75NTR reduces peripheral expansion and CNS trafficking of pro-inflammatory monocytes and spares function after traumatic brain injury. *Journal of Neuroinflammation*, 13(1), 88. <https://doi.org/10.1186/s12974-016-0544-4>
- Lim, S.-H., Park, E., You, B., Jung, Y., Park, A.-R., Park, S. G., & Lee, J.-R. (2013). Neuronal synapse formation induced by microglia and interleukin 10. *PLoS One*, 8(11), e81218. <https://doi.org/10.1371/journal.pone.0081218>
- Luo, C., Zhong, X.-L., Zhou, F. H., Li, J.-Y., Zhou, P., Xu, J.-M., ... Dai, R.-P. (2016). Peripheral brain derived neurotrophic factor precursor regulates pain as an inflammatory mediator. *Scientific Reports*, 6, 27171. <https://doi.org/10.1038/srep27171>
- Meeker, R., & Williams, K. (2014). Dynamic nature of the p75 neurotrophin receptor in response to injury and disease. *Journal of Neuroimmune Pharmacology*, 9(5), 615–628. <https://doi.org/10.1007/s11481-014-9566-9>
- Minnone, G., de Benedetti, F., & Bracci-Laudiero, L. (2017). NGF and its receptors in the regulation of inflammatory response. *International Journal of Molecular Sciences*, 18(5), 1028. <https://doi.org/10.3390/ijms18051028>
- Möhle, L., Israel, N., Paarmann, K., Krohn, M., Pietkiewicz, S., Müller, A., ... Dunay, I. R. (2016). Chronic toxoplasma gondii infection enhances β -amyloid phagocytosis and clearance by recruited monocytes. *Acta Neuropathologica Communications*, 4, 25. <https://doi.org/10.1186/s40478-016-0293-8>
- Möhle, L., Parlog, A., Pahnke, J., & Dunay, I. R. (2014). Spinal cord pathology in chronic experimental toxoplasma gondii infection. *European Journal of Microbiology & Immunology*, 4(1), 65–75. <https://doi.org/10.1556/EuJMI.4.2014.1.6>
- Montoya, J. G., & Liesenfeld, O. (2004). Toxoplasmosis. *Lancet*, 363, 1965e1976.
- Morgan, B., Thorpe, L. W., Marchetti, D., & Perez-Polo, J. R. (1989). Expression of nerve growth factor receptors by human peripheral blood mononuclear cells. *Journal of Neuroscience Research*, 23(1), 41–45. <https://doi.org/10.1002/jnr.490230106>
- Munoz, M., Liesenfeld, O., & Heimesaat, M. M. (2011). Immunology of toxoplasma gondii. *Immunological Reviews*, 240(1), 269–285. <https://doi.org/10.1111/j.1600-065X.2010.00992.x>
- Neumann, H., Misgeld, T., Matsumuro, K., & Wekerle, H. (1998). Neurotrophins inhibit major histocompatibility class II inducibility of microglia: Involvement of the p75 neurotrophin receptor. *Proceedings of the National Academy of Sciences of the United States of America*, 95(10), 5779–5784.
- Nykjaer, A., Willnow, T. E., & Petersen, C. M. (2005). p75NTR—live or let die. *Current Opinion in Neurobiology*, 15(1), 49–57. <https://doi.org/10.1016/j.conb.2005.01.004>
- Orefice, L. L., Shih, C.-C., Xu, H., Waterhouse, E. G., & Xu, B. (2016). Control of spine maturation and pruning through proBDNF synthesized and released in dendrites. *Molecular and Cellular Neurosciences*, 71, 66–79. <https://doi.org/10.1016/j.mcn.2015.12.010>
- Parlog, A., Harsan, L.-A., Zagrebelsky, M., Weller, M., von Elverfeldt, D., Mawrin, C., ... Dunay, I. R. (2014). Chronic murine toxoplasmosis is defined by subtle changes in neuronal connectivity. *Disease Models & Mechanisms*, 7(4), 459–469. <https://doi.org/10.1242/dmm.014183>
- Parlog, A., Schlüter, D., & Dunay, I. R. (2015). Toxoplasma gondii-induced neuronal alterations. *Parasite Immunology*, 37(3), 159–170. <https://doi.org/10.1111/pim.12157>
- Pizzi, M., Sarnico, I., Boroni, F., Benarese, M., Dreano, M., Garotta, G., ... Spano, P. (2004). Prevention of neuron and oligodendrocyte degeneration by interleukin-6 (IL-6) and IL-6 receptor/IL-6 fusion protein in organotypic hippocampal slices. *Molecular and Cellular Neurosciences*, 25(2), 301–311. <https://doi.org/10.1016/j.mcn.2003.10.022>
- Qiao, H., An, S.-C., Xu, C., & Ma, X.-M. (2017). Role of proBDNF and BDNF in dendritic spine plasticity and depressive-like behaviors induced by an animal model of depression. *Brain Research*, 1663, 29–37. <https://doi.org/10.1016/j.brainres.2017.02.020>
- Rauskolb, S., Zagrebelsky, M., Dreznjak, A., Deogracias, R., Matsumoto, T., Wiese, S., ... Barde, Y.-A. (2010). Global deprivation of brain-derived neurotrophic factor in the CNS reveals an area-specific requirement for dendritic growth. *The Journal of Neuroscience: The Official Journal of the Society for Neuroscience*, 30(5), 1739–1749. <https://doi.org/10.1523/JNEUROSCI.5100-09.2010>
- Samah, B., Porcheray, F., & Gras, G. (2008). Neurotrophins modulate monocyte chemotaxis without affecting macrophage function. *Clinical and Experimental Immunology*, 151(3), 476–486. <https://doi.org/10.1111/j.1365-2249.2007.03578.x>
- Schack, D. v., Casademunt, E., Schweigreiter, R., Meyer, M., Bibel, M., & Dechant, G. (2001). Complete ablation of the neurotrophin receptor p75NTR causes defects both in the nervous and the vascular system. *Nature Neuroscience*, 4, 977–978. <https://doi.org/10.1038/nn730>
- Scheller, J., Chalaris, A., Schmidt-Arras, D., & Rose-John, S. (2011). The pro- and anti-inflammatory properties of the cytokine interleukin-6. *Biochimica et Biophysica Acta*, 1813(5), 878–888. <https://doi.org/10.1016/j.bbamcr.2011.01.034>
- Schindelin, J., Arganda-Carreras, I., Frise, E., Kaynig, V., Longair, M., Pietzsch, T., ... Cardona, A. (2012). Fiji: An open-source platform for biological-image analysis. *Nature Methods*, 9(7), 676–682. <https://doi.org/10.1038/nmeth.2019>
- Schlüter, D., Deckert-Schlüter, M., Lorenz, E., Meyer, T., Röllinghoff, M., & Bogdan, C. (1999). Inhibition of inducible nitric oxide synthase exacerbates chronic cerebral toxoplasmosis in toxoplasma gondii-susceptible C57BL/6 mice but does not reactivate the latent disease in T. gondii-resistant BALB/c mice. *The Journal of Immunology*, 162(6), 3512–3518. Retrieved from <http://www.jimmunol.org/content/162/6/3512.short>



- Sholl, D. A. (1953). Dendritic organization in the neurons of the visual and motor cortices of the cat. *Journal of Anatomy*, 87, 387–406.
- Stephens, R. M., Loeb, D. M., Copeland, T. D., Pawson, T., Greene, L. A., & Kaplan, D. R. (1994). Trk receptors use redundant signal transduction pathways involving SHC and PLC- γ 1 to mediate NGF responses. *Neuron*, 12(3), 691–705. [https://doi.org/10.1016/0896-6273\(94\)90223-2](https://doi.org/10.1016/0896-6273(94)90223-2)
- Tilg, H., Dinarello, C. A., & Mier, J. W. (1997). IL-6 and APPs: Anti-inflammatory and immunosuppressive mediators. *Immunology Today*, 18(9), 428–432. [https://doi.org/10.1016/S0167-5699\(97\)01103-1](https://doi.org/10.1016/S0167-5699(97)01103-1)
- Vega, J. A., Garcia-Suarez, O., Hannestad, J., Perez-Perez, M., & Germana, A. (2003). Neurotrophins and the immune system. *Journal of Anatomy*, 203(1), 1–19. <https://doi.org/10.1046/j.1469-7580.2003.00203.x>
- Vyas, A., Kim, S.-K., Giacomini, N., Boothroyd, J. C., & Sapolsky, R. M. (2007). Behavioral changes induced by toxoplasma infection of rodents are highly specific to aversion of cat odors. *Proceedings of the National Academy of Sciences of the United States of America*, 104(15), 6442–6447. <https://doi.org/10.1073/pnas.0608310104>
- Williams, K. S., Killebrew, D. A., Clary, G. P., Seawell, J. A., & Meeker, R. B. (2015). Differential regulation of macrophage phenotype by mature and pro-nerve growth factor. *Journal of Neuroimmunology*, 285, 76–93. <https://doi.org/10.1016/j.jneuroim.2015.05.016>
- Wilson, E. H., & Hunter, C. A. (2004). The role of astrocytes in the immunopathogenesis of toxoplasmic encephalitis. *International Journal for Parasitology*, 34(5), 543–548. <https://doi.org/10.1016/j.ijpara.2003.12.010>
- Wong, I., Liao, H., Bai, X., Zaknic, A., Zhong, J., Guan, Y., ... Zhou, X.-F. (2010). ProBDNF inhibits infiltration of ED1+ macrophages after spinal cord injury. *Brain, Behavior, and Immunity*, 24(4), 585–597. <https://doi.org/10.1016/j.bbi.2010.01.001>
- Woo, N. H., Teng, H. K., Siao, C.-J., Chiaruttini, C., Pang, P. T., Milner, T. A., ... Lu, B. (2005). Activation of p75^{NTR} by proBDNF facilitates hippocampal long-term depression. *Nature Neuroscience*, 8(8), 1069–1077. <https://doi.org/10.1038/nn1510>
- Wood, J. A., Wood, P. L., Ryan, R., Graff-Radford, N. R., Pilapil, C., Robitaille, Y., & Quirion, R. (1993). Cytokine indices in Alzheimer's temporal cortex: No changes in mature IL-1 β or IL-1RA but increases in the associated acute phase proteins IL-6, α 2-macroglobulin and C-reactive protein. *Brain Research*, 629(2), 245–252. [https://doi.org/10.1016/0006-8993\(93\)91327-O](https://doi.org/10.1016/0006-8993(93)91327-O)
- Xie, Y., Tisi, M. A., Yeo, T. T., & Longo, F. M. (2000). Nerve growth factor (NGF) loop 4 dimeric mimetics activate ERK and AKT and promote NGF-like neurotrophic effects. *Journal of Biological Chemistry*, 275(38), 29868–29874. <https://doi.org/10.1074/jbc.M005071200>
- Xing, Z., Gauldie, J., Cox, G., Baumann, H., Jordana, M., Lei, X. F., & Achong, M. K. (1998). IL-6 is an antiinflammatory cytokine required for controlling local or systemic acute inflammatory responses. *The Journal of Clinical Investigation*, 101(2), 311–320. <https://doi.org/10.1172/JCI1368>
- Yang, J., Harte-Hargrove, L. C., Siao, C.-J., Marinic, T., Clarke, R., Ma, Q., ... Hempstead, B. L. (2014). proBDNF negatively regulates neuronal remodeling, synaptic transmission, and synaptic plasticity in hippocampus. *Cell Reports*, 7(3), 796–806. <https://doi.org/10.1016/j.celrep.2014.03.040>
- Yap, G. S., Schariton-Kersten, T., Charest, H., & Sher, A. (1998). Decreased resistance of TNF receptor p55- and p75-deficient mice to chronic toxoplasmosis despite normal activation of inducible nitric oxide synthase in vivo. *The Journal of Immunology*, 160(3), 1340–1345.
- Zagrebel'sky, M., Holz, A., Dechant, G., Barde, Y.-A., Bonhoeffer, T., & Korte, M. (2005). The p75 neurotrophin receptor negatively modulates dendrite complexity and spine density in hippocampal neurons. *The Journal of Neuroscience: the Official Journal of the Society for Neuroscience*, 25, 9989–9999. <https://doi.org/10.1523/JNEUROSCI.2492-05.2005>
- Zagrebel'sky, M., & Korte, M. (2014). Form follows function: BDNF and its involvement in sculpting the function and structure of synapses. *Neuropharmacology*, 76(Pt C), 628–638. <https://doi.org/10.1016/j.neuropharm.2013.05.029>

SUPPORTING INFORMATION

Additional supporting information may be found online in the Supporting Information section at the end of the article.

How to cite this article: Düsedau HP, Klevevan J, Figueiredo CA, et al. p75^{NTR} regulates brain mononuclear cell function and neuronal structure in *Toxoplasma* infection-induced neuroinflammation. *Glia*. 2019;67:193–211. <https://doi.org/10.1002/glia.23553>